

Improving the Foundation Layers for Concrete Pavements

TECHNICAL REPORT:

Jointed Concrete Pavement Rehabilitation with Precast Concrete Pavement – California I-15 Field Study



March 2016

Sponsored by

Federal Highway Administration (DTFH 61-06-H-00011 (Work Plan #18))

FHWA TPF-5(183): California, Iowa (lead state), Michigan, Pennsylvania, Wisconsin

National Concrete Pavement
Technology Center



CENTER FOR

CEER

EARTHWORKS ENGINEERING
RESEARCH

IOWA STATE UNIVERSITY
Institute for Transportation

About the National CP Tech Center

The mission of the National Concrete Pavement Technology (CP Tech) Center is to unite key transportation stakeholders around the central goal of advancing concrete pavement technology through research, tech transfer, and technology implementation.

About CEER

The mission of the Center for Earthworks Engineering Research (CEER) at Iowa State University is to be the nation's premier institution for developing fundamental knowledge of earth mechanics, and creating innovative technologies, sensors, and systems to enable rapid, high quality, environmentally friendly, and economical construction of roadways, aviation runways, railroad embankments, dams, structural foundations, fortifications constructed from earth materials, and related geotechnical applications.

Disclaimer Notice

The contents of this report reflect the views of the authors, who are responsible for the facts and the accuracy of the information presented herein. The opinions, findings and conclusions expressed in this publication are those of the authors and not necessarily those of the sponsors.

The sponsors assume no liability for the contents or use of the information contained in this document. This report does not constitute a standard, specification, or regulation.

The sponsors do not endorse products or manufacturers. Trademarks or manufacturers' names appear in this report only because they are considered essential to the objective of the document.

Iowa State University Non-Discrimination Statement

Iowa State University does not discriminate on the basis of race, color, age, ethnicity, religion, national origin, pregnancy, sexual orientation, gender identity, genetic information, sex, marital status, disability, or status as a U.S. veteran. Inquiries regarding non-discrimination policies may be directed to Office of Equal Opportunity, Title IX/ADA Coordinator, and Affirmative Action Officer, 3350 Beardshear Hall, Ames, Iowa 50011, 515-294-7612, email eooffice@iastate.edu.

Iowa Department of Transportation Statements

Federal and state laws prohibit employment and/or public accommodation discrimination on the basis of age, color, creed, disability, gender identity, national origin, pregnancy, race, religion, sex, sexual orientation or veteran's status. If you believe you have been discriminated against, please contact the Iowa Civil Rights Commission at 800-457-4416 or the Iowa Department of Transportation affirmative action officer. If you need accommodations because of a disability to access the Iowa Department of Transportation's services, contact the agency's affirmative action officer at 800-262-0003.

The preparation of this report was financed in part through funds provided by the Iowa Department of Transportation through its "Second Revised Agreement for the Management of Research Conducted by Iowa State University for the Iowa Department of Transportation" and its amendments.

The opinions, findings, and conclusions expressed in this publication are those of the authors and not necessarily those of the Iowa Department of Transportation or the U.S. Department of Transportation Federal Highway Administration.

Technical Report Documentation Page

1. Report No. DTFH 61-06-H-00011 Work Plan 18	2. Government Accession No.	3. Recipient's Catalog No.	
4. Title and Subtitle Improving the Foundation Layers for Concrete Pavements: Jointed Concrete Pavement Rehabilitation with Precast Concrete Pavement – California I-15 Field Study	5. Report Date March 2016		6. Performing Organization Code
	7. Author(s) David J. White, Pavana Vennapusa, Yang Zhang		
9. Performing Organization Name and Address National Concrete Pavement Technology Center and Center for Earthworks Engineering Research (CEER) Iowa State University 2711 South Loop Drive, Suite 4700 Ames, IA 50010-8664	8. Performing Organization Report No. InTrans Project 09-352		
	10. Work Unit No. (TRAIS)		
12. Sponsoring Organization Name and Address Federal Highway Administration U.S. Department of Transportation 1200 New Jersey Avenue SE Washington, DC 20590	11. Contract or Grant No.		
	13. Type of Report and Period Covered Technical Report		
14. Sponsoring Agency Code TPF-5(183)			
15. Supplementary Notes Visit www.cptechcenter.org or www.ceer.iastate.edu for color PDF files of this and other research reports.			
16. Abstract This report is one of the field project reports developed as part of the TPF-5(183) and FHWA DTFH 61-06-H-00011:WO18 studies. Precast concrete pavement (PCP) systems can be an effective and safe repair/rehabilitation alternative to cast-in-place pavements for projects in urban area highways with high traffic volumes where lane closures are a significant challenge. Based on these advantages and the success observed from accelerated pavement testing at a test site with PCP in San Bernardino, California, CalTrans opted for PCP rehabilitation over a four-mile section of I-15 near Ontario, California. The rehabilitation work involved removing an existing pavement built in the 1970s and replacing with PCP panels. The existing pavement consisted of portland cement concrete (PCC) pavement over cement treated base. PCPs were placed over 1.8 miles of the project and 34 intermittent panels. The total bid cost of the project was about \$51.9 million. PCP systems constituted approximately \$4.6 million of the total construction cost. Results of field testing and observations by the SHRP2 R05 and CalTrans and the Iowa State University (ISU) research team are summarized in this report. Results indicated that sections with PCP panels showed lower surface deflection values under falling weight deflectometer (FWD) loading than sections with the old pavement. Presence of bedding grout beneath the PCP panels reduced the surface deflections under FWD loading and showed less variability. PCP panels showed thin hair-line cracks several months after placement and the cracked panels correlated well with areas that had problems with placement and leveling of the bedding material. FWD testing conducted on the cement treated base (CTB) layer beneath the pavement layer showed that the CTB layer had an average moduli of over 7,200 MPa and subgrade layer had an average modulus of about 105 MPa and R-value of about 45.			
17. Key Words concrete pavement—pavement foundation—quality assurance—quality control— precast pavement—subbase—subgrade		18. Distribution Statement No restrictions.	
19. Security Classification (of this report) Unclassified.	20. Security Classification (of this page) Unclassified.	21. No. of Pages 53	22. Price NA

**IMPROVING THE FOUNDATION LAYERS
FOR CONCRETE PAVEMENTS:
JOINTED CONCRETE PAVEMENT REHABILITATION
WITH PRECAST CONCRETE PAVEMENT –
CALIFORNIA I-15 FIELD STUDY**

Technical Report
March 2016

Research Team Members

Tom Cackler, David J. White, Jeffrey R. Roesler, Barry Christopher, Andrew Dawson,
Heath Gieselman, and Pavana Vennapusa

Report Authors

David J. White, Pavana K. R. Vennapusa, Yang Zhang
Iowa State University

Sponsored by

the Federal Highway Administration (FHWA)
DTFH61-06-H-00011 Work Plan 18
FHWA Pooled Fund Study TPF-5(183): California, Iowa (lead state),
Michigan, Pennsylvania, Wisconsin

Preparation of this report was financed in part
through funds provided by the Iowa Department of Transportation
through its Research Management Agreement with the
Institute for Transportation
(InTrans Project 09-352)

**National Concrete Pavement Technology Center and
Center for Earthworks Engineering Research (CEER)**

Iowa State University
2711 South Loop Drive, Suite 4700
Ames, IA 50010-8664
Phone: 515-294-8103
www.cptechcenter.org and www.ceer.iastate.edu

TABLE OF CONTENTS

ACKNOWLEDGMENTS	ix
LIST OF ACRONYMS AND SYMBOLS.....	xi
EXECUTIVE SUMMARY	xiii
CHAPTER 1. INTRODUCTION.....	1
CHAPTER 2. OVERVIEW OF PCP SYSTEMS.....	2
CHAPTER 3. PROJECT OVERVIEW AND FIELD TESTING	4
Project Overview	4
Construction Process.....	5
Post Construction Testing and Monitoring.....	9
SHRP 2 R05 Testing.....	9
CalTrans Monitoring.....	10
ISU Field Testing.....	11
CHAPTER 4. TESTING METHODS AND DATA ANALYSIS.....	13
Kuab Falling Weight Deflectometer.....	13
Dynamic Cone Penetrometer	20
Determination of R values	20
Geostatistical Data Analysis	21
CHAPTER 5. RESULTS AND ANALYSIS.....	23
TS1: CTB Layer.....	23
TS2 and TS3: New PCP and Old Pavement	28
CHAPTER 6. SUMMARY AND CONCLUSIONS	34
REFERENCES	37
APPENDIX: CORRELATIONS BETWEEN R-VALUE AND MODULUS	39

LIST OF FIGURES

Figure 1. Removal of existing pavement (June 28, 2010)	5
Figure 2. CTB layer after removal of pavement (June 28, 2010)	6
Figure 3. Bedding sand layer placed on CTB and compacted using a hand operated grader (June 28, 2010).....	7
Figure 4. Installing dowel grout (June 28, 2010).....	8
Figure 5. Two views of installing bedding grout (June 28, 2010).....	8
Figure 6. FWD center plate deflections at mid-panel under 9,000 lb load on I-15 project site (Tayabji et al. 2013a).....	10
Figure 7. FWD center plate deflections near joint under 9,000 lb load on I-15 project site (Tayabji et al. 2013a)	10
Figure 8. Coring operations on CTB layer by ISU research team (June 28, 2010).....	12
Figure 9. Kuab FWD during testing on the site (left) and ISU researchers conducting a DCP test (right).....	13
Figure 10. FWD deflection sensor setup used for this study and a sample deflection basin data illustrating SCI, BDI, and BCI calculations	14
Figure 11. Void detection using load-deflection data from FWD test.....	16
Figure 12. Static k_{PLT} values versus $k_{FWD-Dynamic}$ measurements reported in literature	19
Figure 13. Description and parameters of a typical experimental and spherical semivariogram.....	21
Figure 14. TS1 CTB: Kriged spatial contour map (top), measurements longitudinally along the test section (middle), histogram (bottom left), and semivariogram (bottom right) of E_{FWD-K3} measurements	24
Figure 15. TS1 CTB: Kriged spatial contour map (top), measurements longitudinally along the test section (middle), histogram (bottom left), and semivariogram (bottom right) of E_{SB} (CTB layer modulus) measurements.....	25
Figure 16. TS1 CTB: Kriged spatial contour map (top), measurements longitudinally along the test section (middle), histogram (bottom left), and semivariogram (bottom right) of E_{SG} (subgrade layer modulus) measurements	26
Figure 17. TS1 CTB: Kriged spatial contour map (top), measurements longitudinally along the test section (middle), histogram (bottom left), and semivariogram (bottom right) of R-value measurements.....	27
Figure 18. TS1 CTB: DCP-CBR and cumulative blows with depth profiles at 5 test locations	28
Figure 19. TS2 and TS3: FWD D_0 and joint LTE.....	29
Figure 20. TS2 and TS3: FWD k values and R-value calculated from k value per PCA 1984	29
Figure 21. TS2 and TS3: FWD deflection basin parameters	30
Figure 22. TS2 and TS3: Box plots comparing measurements on new PCP and old pavement for tests conducted near mid-panel: (a) D_0 , (b) I-value, (c) $k_{FWD-Static-Corr}$, (d) SCI, (e) BDI, (f) BCI, (g) Area Factor, and (h) R-value	31
Figure 23. TS2 and TS3: Box plots comparing measurements on new PCP and old pavement for tests conducted near joint: (a) D_0 , (b) LTE, (c) SCI, (d) BDI, (e) BCI, and (f) Area Factor	32
Figure 24. Chart to estimate resilient modulus (M_r) of subgrade from CBR (from AASHTO 1993 Appendix FF based on results from van Til et al. 1972)	39

LIST OF TABLES

Table 1. Summary of test sections and in situ testing.....	12
Table 2. Summary of t-test analysis on FWD deflection basin parameters near mid-panel on new versus old pavement.....	33
Table 3. Summary of t-test analysis on FWD deflection basin parameters near joint on new and old pavement	33

ACKNOWLEDGMENTS

This research was conducted under Federal Highway Administration (FHWA) DTFH61-06-H-00011 Work Plan 18 and the FHWA Pooled Fund Study TPF-5(183), involving the following state departments of transportation:

- California
- Iowa (lead state)
- Michigan
- Pennsylvania
- Wisconsin

The authors would like to express their gratitude to the National Concrete Pavement Technology (CPTech) Center, the FHWA, the Iowa Department of Transportation (DOT), and the other pooled fund state partners for their financial support and technical assistance.

Mehdi Parvini with CalTrans and several field engineers with CalTrans have provided assistance in identifying the project, providing access to the project site, and obtaining project design information. We greatly appreciate their help.

We also thank Rachel Franz of Iowa State University for her help with laboratory and field testing; and Christianna White for comments and editing support.

LIST OF SYMBOLS AND ACRONYMS

BCI	Base curvature index
BDI	Base damage index
CBR	California bearing ratio
COV	Coefficient of variation
CTB	Cement treated base
D_0	Deflection measured under the plate
D_0^*	Non-dimensional deflection coefficient
D_1 to D_7	Deflections measured away from the plate at various set distances
DCP	Dynamic cone penetrometer
E_{SB}	Elastic modulus of the CTB layer
E_{SG}	Elastic modulus of the subgrade layer
E_{FWD-K3}	Composite elastic modulus determined from FWD test
FWD	Falling weight deflectometer
F	shape factor depending on stress distribution
h	Separation distance
I	Intercept
k	Modulus of subgrade reaction
$k_{FWD-Dynamic}$	Dynamic modulus of subgrade reaction from FWD test
$k_{FWD-Static}$	Static modulus of subgrade reaction from FWD test
$k_{FWD-Static-Corr}$	Static modulus of subgrade reaction from FWD test corrected for finite slab size
L	Relative stiffness
LTE	Load transfer efficiency
n	Number of measurements
P	Applied load
PCC	Portland cement concrete
PCP	Precast concrete panel
r	Plate radius
R	R or Stabilometer test value
SCI, BCI, BDI, AF	FWD deflection basin parameters
T_L	Equivalent linear temperature gradients
μ	Statistical mean or average
η	Poisson's ratio
σ	Statistical standard deviation
σ_0	Applied stress
$\gamma(h)$	Semivariogram function

EXECUTIVE SUMMARY

Quality foundation layers (the natural subgrade, subbase, and embankment) are essential to achieving excellent pavement performance. Unfortunately, many pavements in the United States still fail due to inadequate foundation layers. To address this problem, a research project, Improving the Foundation Layers for Pavements (FHWA DTFH 61-06-H-00011 WO #18; FHWA TPF-5(183)), was undertaken by Iowa State University to identify, and provide guidance for implementing, best practices regarding foundation layer construction methods, material selection, in situ testing and evaluation, and performance-related designs and specifications. As part of the project, field studies were conducted on several in-service concrete pavements across the country that represented either premature failures or successful long-term pavements. A key aspect of each field study was to tie performance of the foundation layers to key engineering properties and pavement performance. In situ foundation layer performance data, as well as original construction data and maintenance/rehabilitation history data, were collected and geospatially and statistically analyzed to determine the effects of site-specific foundation layer construction methods, site evaluation, materials selection, design, treatments, and maintenance procedures on the performance of the foundation layers and of the related pavements. A technical report was prepared for each field study.

Precast concrete pavement (PCP) systems are pre-fabricated concrete panels that are fabricated off-site, transported to project site, and placed in situ on prepared foundations after removal of existing pavements. PCPs can be an effective and safe repair/rehabilitation alternative to cast-in-place pavements on projects in urban area highways with high traffic volumes where lane closures are a significant challenge.

Based on these advantages and the success observed from accelerated pavement testing at a test site with PCP in San Bernardino, California, CalTrans opted for PCP rehabilitation over a 4-mile section of I-15 near Ontario, California. The rehabilitation work involved removing an existing pavement built in the 1970s and replacing with PCP panels. The existing pavement consisted of nominal 213 mm (8.4 in.) of PCC over 122 mm (4.8 in. of CTB). PCPs were placed over 1.8 miles of the project and 34 intermittent panels. The total bid cost of the project was about \$51.9 million. PCP systems constituted approximately \$4.6 million of the total construction cost.

The rehabilitation process involved removing the old pavement, placing a new thin bedding sand layer was placed, placing 203 mm (8 in.) thick new PCP panels, and pumping bedding and dowel slot grouts. Bedding grout was pumped into precast ports for undersealing and dowel grout was injected to the dowel slots.

Preliminary field testing using falling weight deflectometer (FWD) was conducted on this project as part of a research effort by SHRP2 R05 in early June 2010. Crack monitoring was performed by CalTrans several months after the construction completed and opened to traffic. The Iowa State University (ISU) research team was present on-site on June 28, 2010 to monitor construction operations and conduct field testing. Kuab FWD and dynamic cone penetrometer (DCP) tests were conducted on CTB layer, and FWD tests were conducted on two adjacent test sections consisting of old pavement and new PCP panels.

Following are some key findings from work performed by the SHRP2 R05 research team and CalTrans:

- FWD testing was conducted by Tayabji et al. (2013a) on PCP panels constructed with and without bedding grout. The results showed that deflections were considerably smaller (3 to 5 mils) on panels where bedding grout was used.
- The panels with only dowel-slot grouting showed more variability in surface deflections.
- Field monitoring several months after construction showed thin hair-line cracks on several panels. A detailed survey was conducted on 696 panels, of which 24% were cracked.
- Based on crack survey mapping and field notes during construction, it was concluded that the contractor's grading practices contributed to the cracking. It was found that the stringline approach used to place the bedding material sometimes created high and low spots resulting in non-uniform support conditions. Cracks at some locations were attributed to opening the lane to traffic before grouting.

The ISU research team was present on site on June 28, 2010 to monitor construction operations and conduct field testing. Kuab FWD and DCP tests were conducted on CTB layer, and FWD tests were conducted on two adjacent test sections consisting of old pavement and new PCP panels. Following are some key findings from the ISU testing:

- Tests on the CTB layer indicated that the average composite modulus was about 357 MPa with a COV of about 17%. The average CTB layer modulus was about 7,200 MPa with a COV of about 42%. The average subgrade layer modulus was about 105 MPa with a COV of about 10%, which represented relatively stiff subgrade conditions.
- CBR values estimated in the subgrade from DCP tests showed relatively high values (ranging between 30 and 100), which confirms the relatively high subgrade modulus values. The average R-value of the subgrade was about 45 with a COV of about 5%.
- Statistical analysis of FWD measurement values obtained on the old and new pavement indicated that there was a statistically significant difference in surface deflection (D_0) and zero-load intercept (I) values near mid-panel, but not in any of the other deflection basin parameters and the modulus of subgrade reaction (k) value. The D_0 and I values were lower on the new pavement than on the old pavement. This suggests that there was improvement in the deflection response near the surface, which reflects better support conditions directly beneath the new pavement. This was also confirmed in the SHRP2 R05 testing. Deeper improvements are not expected which is reflected in the deflection basin parameters.
- There were no statistically significant differences in any of the measurement values obtained at the joint. The LTE values were relatively high (> 85%) at all locations.
- The average R-value obtained from FWD testing was about 50 and was similar to the value obtained from FWD testing on the CTB layer (45).

CHAPTER 1. INTRODUCTION

Precast concrete pavement (PCP) systems are pre-fabricated concrete panels that are fabricated off-site, transported to project site, and placed in situ on prepared foundation after removal of the existing pavement. PCPs can be an effective and safe repair/rehabilitation alternative to cast-in-place pavements on projects in urban area highways with high traffic volumes where lane closures is a significant challenge.

Based on these advantages and the success observed from accelerated pavement testing at a test site with PCP in San Bernardino, California, CalTrans opted for PCP rehabilitation over a 4 mile section of I-15 near Ontario, California. The rehabilitation work involved removing an existing pavement built in the 1970s and replacing with precast concrete pavement (PCP) panels. The existing pavement consisted of nominal 213 mm (8.4 in.) of PCC over 122 mm (4.8 in. of CTB). PCPs were placed over 1.8 miles of the project and 34 intermittent panels. The total bid cost of the project was about \$51.9 million. PCP systems constituted approximately \$4.6 million of the total construction cost.

Preliminary field testing using a falling weight deflectometer (FWD) was conducted on this project as part of a research effort by SHRP2 R05 (Tayabji et al. 2013b) in early June 2010. Crack monitoring was performed by CalTrans several months after construction was completed and the road was opened to traffic. The Iowa State University (ISU) research team was present on-site on June 28, 2010, to monitor construction operations and conduct Kuab FWD and dynamic cone penetrometer testing. Both DCP and FWD tests were conducted on the CTB layer, and FWD tests were conducted on sections with old pavement and new PCP panels.

FWD testing was conducted on the CTB layer to evaluate the modulus values of the CTB layer and the underlying subgrade layer. FWD testing on the pavement layers was conducted to evaluate differences in surface deflections and deflection basin parameters between the old pavement and the new pavement panels.

Chapter 2 of this report presents an overview of PCP systems. Chapter 3 provides a project overview and results of initial field testing and the ISU testing plan. Chapter 4 summarizes the test methods and data analysis methods. Chapter 5 presents the results and analysis from this study.

CHAPTER 2. OVERVIEW OF PCP SYSTEMS

Precast concrete pavement (PCP) systems consist of pre-fabricated concrete panels that are fabricated off-site, transported to project sites, and placed in situ on prepared foundations after removal of existing pavement. PCP applications include isolated repairs such as patching work, intersection and ramp rehabilitation, urban street rehabilitation, and rehabilitation of longer mainline pavement sections (Tayabji et al. 2013b). PCP construction can be an effective and safe repair/rehabilitation alternative to cast-in-place pavements on projects in urban area highways with high traffic volumes where lane closures are a significant challenge. According to Tayabji et al. (2013b), the specific advantages of using PCP versus cast-in-place concrete pavements include the following:

- Better-quality concrete: problems related to concrete delivery or paving equipment operation, including poor concrete quality, concrete consolidation, and over finishing of the concrete surface, are eliminated.
- Better concrete curing conditions: curing of the PCPs takes place under controlled conditions at the plant.
- Minimal weather restrictions on placement: the construction season can be extended because PCPs can be placed in cool weather or during light rainfall.
- Reduced delay before opening to traffic: on-site curing of the concrete is not required. As a result, PCPs can be installed during nighttime lane closures and be ready to be opened to traffic the following morning.
- No joint raveling: Early-age failures due to late or shallow joint sawing are eliminated.

A recent SHRP2 R05 project focused on identifying the different PCP systems and the current state of U.S. and international practices; evaluating performance; developing guidelines for selection, design, fabrication, and installation; and developing model PCP specifications (Tayabji et al. 2013a). As part of that project, field testing and evaluation were conducted on 16 PCP construction projects in the U.S., including the one discussed in this report (California I-15). Tayabji et al. (2013a) concluded that PCP systems are capable of performing well under traffic loading, and the behavior and performance of PCP systems is similar to that of the cast in place concrete pavements. They also indicated that constructability, durability, and performance (with respect to panel support conditions and load transfer at joints) are the key attributes of PCP system that presented concerns to users. According to Tayabji et al. (2013b), sufficient advances have been made on all these aspects to produce a reliable product.

Tayabji et al. (2013a) provided a summary of technical considerations for support conditions when placing PCP systems. They suggested that proper seating of the panels on the base is critical to the design, construction, and long-term performance of the PCP systems. According to Tayabji et al.,

the quality of base and bedding materials must be controlled to ensure that these materials provide the desired support and that the support is uniform along the length of each panel. To date, no serious attempts have been made to control the compaction of granular base or bedding materials by controlling the moisture content of these materials. It is important that

testing of the granular base or bedding, or both, be performed to monitor the compaction level.

A bedding layer is routinely used with PCP systems to ensure uniform support under the panels. If a fine-grained granular bedding material is used, its thickness should be limited to ¼ in. (6 mm). If a thicker bedding layer is necessary, then rapid-setting cementitious grout or flowable fill may be considered. As a general rule, any base or bedding material that would not be allowed during the construction of CIP concrete should not be used with a PCP system.

Finally, if the opportunity does not exist to improve the base or bedding system and the subgrade is of marginal quality, more attention should be paid to the design of the JCP system. The load transfer system at transverse joints must be adequate, and the panels may need to be prestressed if thicker nominally reinforced panels cannot be accommodated. Panels of only one size (thickness) cannot be expected to meet all design needs, especially when marginal support conditions are encountered. (2013a, 60)

CHAPTER 3. PROJECT OVERVIEW AND FIELD TESTING

Project Overview

This project tested in this study (CalTrans EA08-472214) is located on I-15 near Ontario, California. The summary construction report provided by Hartog (2012) was used to develop the following information.

The project limits over a total distance of about 4 miles are from State Route 60 in Riverside County to approximately one mile north of I-10 in San Bernardino County. The total bid cost of the project was about \$51.9 million. PCP systems constituted approximately \$4.6 million of the total construction cost. PCPs were placed over 1.8 miles of the project and 34 intermittent panels, and a total of 730 panels were installed. Unit cost of the PCP for winning bid was about \$418/panel, while the cost of the panels directly from the manufacturer was about \$253. The difference in cost was attributed to contractor's additional cost for removal of existing panels, grading, bedding layer placement, installation of PCPs, and survey work.

The existing pavement was originally constructed in the 1970s with approximately 213 mm (8.4 in.) of PCC over 122 mm (4.8 in. of CTB). The annual average daily traffic (AADT) was about 196,500 per day in 2003 with 6% trucks in the peak hour and a peak hour volume of 16,150 vehicles.

CalTrans based the decision to use PCP layer on this site on the success of accelerated pavement testing performed by the Pavement Research Center at the University of California at a nearby test site in San Bernardino in 2005 and 2006 (Kohler et al. 2007). Testing was performed using a heavy vehicle simulator (HVS) on a test strip of PCP system installed near I-15/I-210 interchange in San Bernardino, California. According to Kohler et al.,

given the design of the pre-cast PCC pavement tested at the San Bernardino test site, the tight control over the construction process, and the favorable HVS test conditions, no premature failure is anticipated with the use of the pre-cast PCC pavement on actual rehabilitation projects. The ultimate structural capacity of the system will probably exceed 40 million ESALS. The structural capacity of the system will, however, have to be determined for a range of support and environmental conditions before it can be used with absolute certainty. (2007, ii)

During the initial phase of the project, cores were taken in the pavement and the underlying CTB layer to assess its conditions and get layer thicknesses. The as-builts indicated that the pavement thickness was 213 mm (8.4 in.). However, Hartog (2012) reported that actual pavement thicknesses varied from 163 mm (6.4 in.) to 271 mm (10.7 in.) although Hartog indicated that the cores taken during the initial phase were not sufficient to capture the observed variations.

Construction Process

The PCPs were cast off-site under controlled conditions indoors using adjustable forms developed by Fort Miller. They were steam cured to prevent shrinkage cracks. Dowel bars, dowel slots, and grouting ports were cast into the panels.

The existing pavements were removed (Figure 1) down to the existing CTB layer (Figure 2) and a thin sand bedding layer consisting of washed concrete sand material was placed on the CTB layer. The bedding layer was compacted using three passes. The first pass was performed by a tractor with a gannon attachment; the second pass was performed by a hand-operated grader (Figure 3); and the third pass was performed by a single pass of a roller.



Figure 1. Removal of existing pavement (June 28, 2010)



Figure 2. CTB layer after removal of pavement (June 28, 2010)



Figure 3. Bedding sand layer placed on CTB and compacted using a hand operated grader (June 28, 2010)

After grading was completed, panels were placed on the bedding material and were set to marks established by the surveyor. Two adjacent panels were not set tight against the other panels to avoid creep issues.

Two types of grout were used on this site, dowel grout and bedding grout. The dowel grout consisted of high-strength grout material that achieved 2,500 psi in 2 hours or less. The grouting process are shown in Figure 4. Bedding grout was injected through a port cast in the panel which travelled through the channels that were cast in the bottom of the panel to a port on the opposite end of the channel. Four bedding grout channels were cast in the bottom of each panel to ensure fairly uniform distribution of the bedding grout. On this project, dowel grouting was performed the night of installation and the bedding grouting was performed the following night. After grouting, the joints were milled and sealed as necessary.



Figure 4. Installing dowel grout (June 28, 2010)

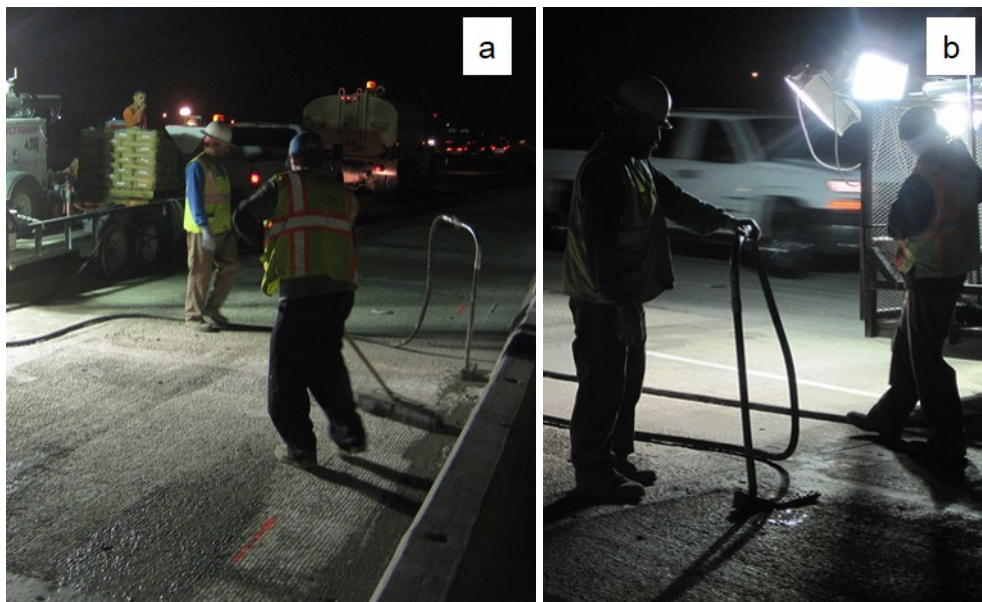


Figure 5. Two views of installing bedding grout (June 28, 2010)

The following is a list of equipment and personnel used to perform the PCP installation on this site (Hartog, 2012):

- 1 hand-operated grader (HOG) used to finish-grade the bedding layer
- 1 skip loader used to place and rough-grade the bedding layer
- 1 water truck used to wet the bedding layer prior to compaction
- 1 steel-tired roller used to compact the bedding layer
- 1 40-ton crane for placing precast panel elements

- 1 concrete saw (sawcutting normally performed the night prior to pcp installation)
- 1 excavator for removing concrete and 1 sweeper
- 1 grinder for milling CTB if existing concrete is thin
- 1 grouting pump and truck to haul and pump grout
- haul trucks for concrete removal, delivery truck for bedding material, and delivery trucks for precast panel elements
- 1 foreman
- 1 crane operator
- 1 excavator/roller operator
- 1 skip loader operator
- 1 grinder operator
- 1 water truck/sweeper operator
- 4 carpenters (for setting the rails that the HOG ran on)
- 1 grout pump operator
- 2 laborers to help with grouting
- 3–4 laborers to operate the HOG
- 3–4 laborers to set panels

Post Construction Testing and Monitoring

SHRP 2 R05 Testing

Tayabji et al. (2013a) conducted FWD testing during the daytime in June 2010 before opening to traffic. The tests were performed on two sections with precast panels. One section consisted of 30 panels with both grouted dowel slots and undersealed with bedding grout (fully grouted panels). The second section consisted of 12 panels with only grouted dowel slots and no bedding grout (dowel only panels). Testing was performed with the objective of comparing deflection response between the two sections. Results are presented in Figure 6 and Figure 7. Test results near mid-panel indicated that the fully grouted panels had an average of 3 mil less deflection than the dowel only panels. Test results near joints indicated that the fully grouted panels had an average of 5 mil less deflection than dowel only panels. Also, the panels with only grouted dowel slots showed more variability in surface deflections.

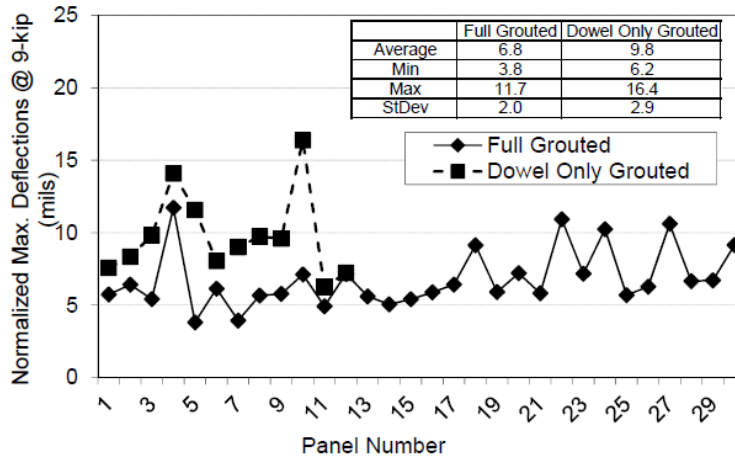


Figure 6. FWD center plate deflections at mid-panel under 9,000 lb load on I-15 project site (Tayabji et al. 2013a)

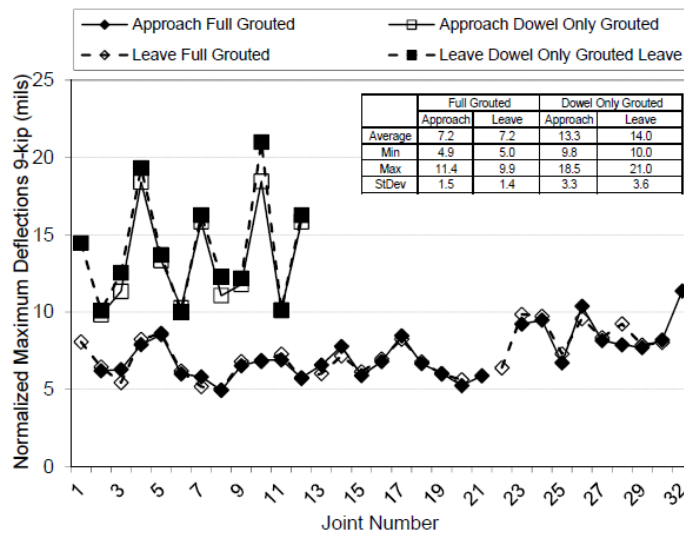


Figure 7. FWD center plate deflections near joint under 9,000 lb load on I-15 project site (Tayabji et al. 2013a)

CalTrans Monitoring

Hartog (2012) summarized field observations several months after the PCPs were cast. Thin hair-line cracks were apparently observed on a number of panels following a rain event. Petrographic analysis of cores suggested that the cracking was structurally related and not shrinkage related and that the quality of the concrete did not contribute to cracking.

Hartog (2012) documented a survey of cracked and uncracked panels in relation to the construction notes in terms of any grading or other issues noted by the contractor. Of the 696

panels surveyed, 24% were cracked. Grading issues were noted by the contractor when placing bedding material using a string line approach that resulted in voids and low/high points underneath panels that created non-uniform support conditions beneath the panel. Other reported issues were occasions when contractors installed panels but opened to traffic without grouting the panels.

Lane 4 (the right most lane) showed more cracked panels (27%) than lane 3, which was attributed to higher truck traffic. The contractor's grading and grouting practices showed strong correlation with the incidence of cracking.

ISU Field Testing

The ISU research team was present on site on June 28, 2010, to monitor construction operations and conduct field Kuab FWD and DCP testing. A summary of test sections is provided in Table 1.

FWD tests were conducted on the existing CTB layer, newly constructed PCPs, and the existing pavement. 100 mm (4 in.) cores were performed in the CTB layer (Figure 8) to extract samples for laboratory testing, but intact samples could not be obtained. DCP tests were conducted in the subgrade layer after the core was removed.

FWD testing was performed in test section 1 (TS1) on the CTB layer in a dense grid pattern over a span of about 33 m at three locations over a width of about 2.5 m, with a total of about 44 tests. In TS2 and TS3, FWD testing was performed near joint and at mid-panel to compare surface deflections and the support conditions between the old and the new pavement slabs. TS2 and TS3 were located in adjacent lanes.

PCP slabs on TS2 were fully grouted at the time of testing with bed grouting and dowel slot grouting.

Table 1. Summary of test sections and in situ testing

TS	Date	Location	Material	Test	Comments
1		About 160 m (500 ft) south of exit 110 on I-15	CTB	DCP, FWD, core drill	Three rows of 15, 14, 16 points heading in north direction, 0.9 m spacing between paths.
2	6/28/10	Lane west of TS1	New slabs	FWD	FWD on in-place slabs. Every other panel – tested center and joint
3		Directly north of TS2	Old slabs	FWD	Old pavement north of new panels, will be replaced with new slabs



Figure 8. Coring operations on CTB layer by ISU research team (June 28, 2010)

CHAPTER 4. TESTING METHODS AND DATA ANALYSIS

This chapter summarizes the field testing methods and statistical data analysis used in this study. The following in situ testing methods and devices were used in this study: a Kuab falling weight deflectometer (FWD) setup with a 300 mm diameter plate and a dynamic cone penetrometer (DCP). Pictures of these test devices are shown in Figure 9.



Figure 9. Kuab FWD during testing on the site (left) and ISU researchers conducting a DCP test (right)

Kuab Falling Weight Deflectometer

Falling weight deflectometer (FWD) tests were conducted using a Kuab FWD setup with a 300 mm (11.81 in) diameter loading plate by applying one seating drop and three loading drops. The applied loads varied from about 27 kN (6,000 lb) to 54 kN (12,000 lb) in the three loading drops. The actual applied loads were recorded using a load cell, and deflections were recorded using seismometers mounted on the device, per ASTM D4694-09 *Standard Test Method for Deflections with a Falling-Weight-Type Impulse Load Device*. The FWD plate and deflection sensor setup and a typical deflection basin are shown in Figure 10. To compare deflection values from different test locations at the same applied contact stress, the values at each test location were normalized to a 40 kN (9,000 lb) applied force.

FWD tests were conducted at the center of the PCC slab panels and at the joints. Tests conducted at the joints were used to determine joint load transfer efficiency (LTE) and voids beneath the pavement based on “zero” load intercept values. Tests conducted at the center of the slab panels were used to determine modulus of subgrade reaction (k) values and the intercept values. The procedure used to calculate these parameters are described below.

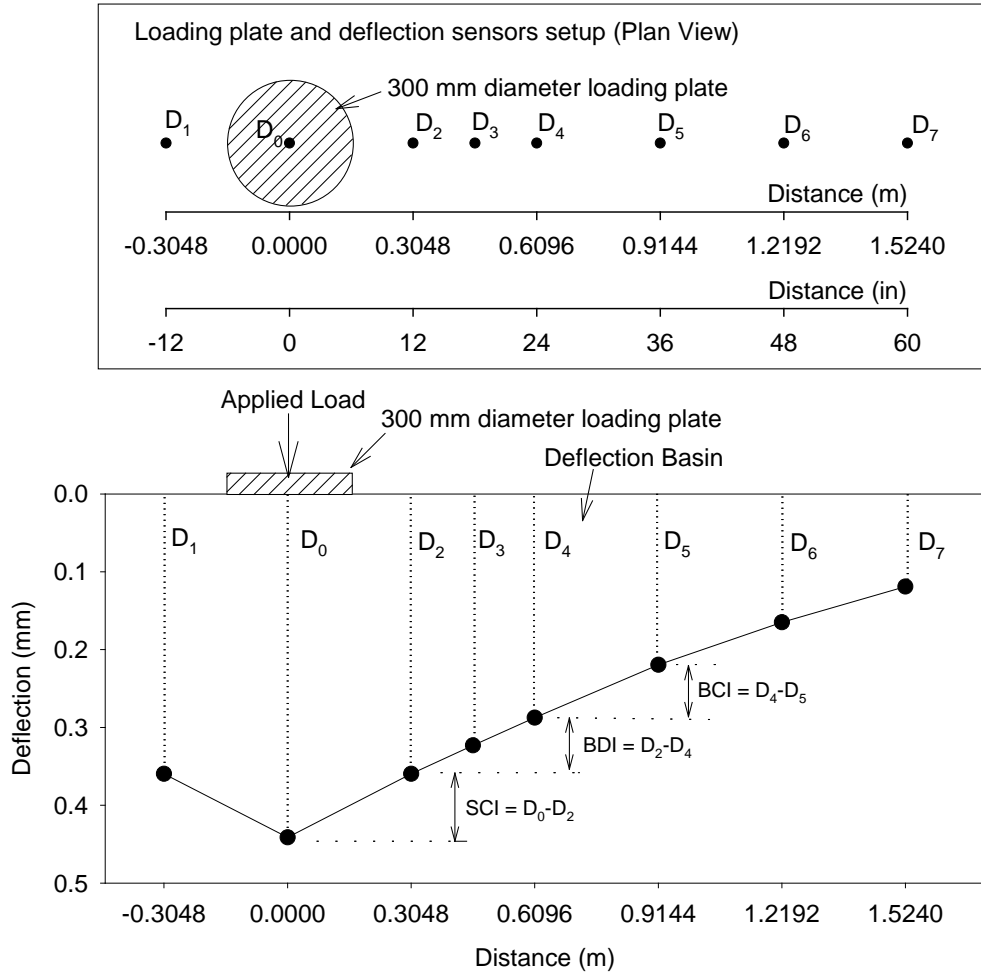


Figure 10. FWD deflection sensor setup used for this study and a sample deflection basin data illustrating SCI, BDI, and BCI calculations

The SCI, BDI, BCI, and AF measurements are referred to as deflection basin parameters and are determined using the following equations:

$$SCI \text{ (mm)} = D_0 - D_2 \quad (5)$$

$$BDI \text{ (mm)} = D_2 - D_4 \quad (6)$$

$$BCI \text{ (mm)} = D_4 - D_5 \quad (7)$$

$$AF \text{ (mm)} = \frac{152.4 \times (D_0 + 2D_2 + 2D_4 + D_5)}{D_0} \quad (8)$$

where, D_0 = peak deflection measured directly beneath the plate, D_2 = peak deflection measured at 305 mm away from the plate center, D_4 = peak deflection measured at 510 mm away from the plate centre, and D_5 = peak deflection measured at 914 mm away from the plate centre.

According to Horak (1987), the SCI parameter provides a measure of the strength/ stiffness of the upper portion (base layers) of the pavement foundation layers (Horak 1987). Similarly, BDI represents layers between 300 mm and 600 mm depth (base and subbase layers) and BCI represents layers between 600 mm and 900 mm depth (subgrade layers) from the surface (Kilareski and Anani 1982). The AF is primarily the normalized (with D_0) area under the deflection basin curve up to sensor D_5 (AASHTO 1993). AF has been used to characterize variations in the foundation layer material properties by some researchers (e.g., Stubstad 2002). Comparatively lower SCI or BDI or BCI or AF values indicate better support conditions (Horak 1987).

LTE was determined by obtaining deflections under the plate on the loaded slab (D_0) and deflections of the unloaded slab (D_1) using a sensor positioned about 305 mm (12 in.) away from the center of the plate (Figure 10). The LTE was calculated using Equation 4.

$$LTE(\%) = \frac{D_1}{D_0} \times 100 \quad (4)$$

Voids underneath pavements can be detected by plotting the applied load measurements on the X-axis and the corresponding deflection measurements on the y-axis and plotting a best fit linear regression line, as illustrated in Figure 11, to determine the “zero” load intercept (I) values. AASHTO (1993) suggests $I = 0.05$ mm (2 mils) as a critical value for void detection. According to van Quintus and Simpson (2002), if $I = -0.01$ and $+0.01$ mm, then the response would be considered elastic. If $I > 0.01$ then the response would be considered deflection hardening, and if $I < -0.01$ then the response would be considered deflection softening.

Pavement layer temperatures at different depths were obtained during FWD testing, in accordance with the guidelines from Schmalzer (2006). The temperature measurements were used to determine equivalent linear temperature gradients (T_L) following the temperature-moment concept suggested by Janssen and Snyder (2000). According to Vandenbossche (2005), I-values are sensitive to temperature induced curling and warping affects. Large positive temperature gradients (i.e., when the surface is warmer than the bottom) that cause the panel corners to curl down result in false negative I-values. Conversely, large negative gradients (i.e., when the surface is cooler than the bottom) that cause the panel corners to curl upward result in false positive I-values. Interpretation of I-values therefore should consider the temperature gradient. Concerning LTE measurements for doweled joints, the temperature gradient is reportedly not a critical factor (Vandenbossche 2005).

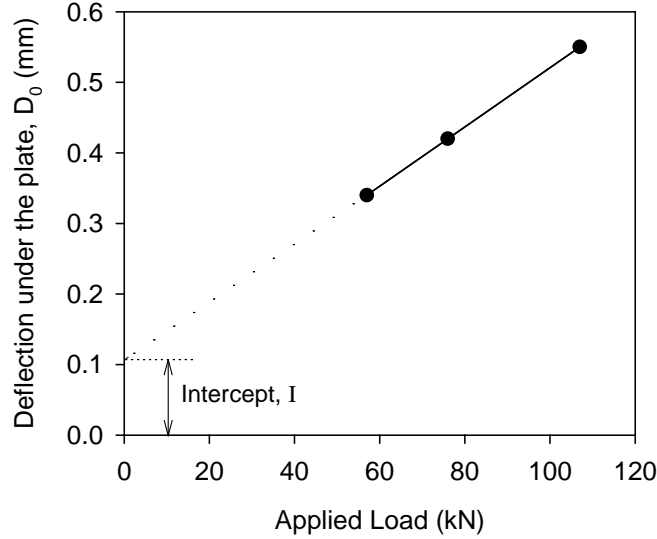


Figure 11. Void detection using load-deflection data from FWD test

The k values were determined using the AREA₄ method described in AASHTO (1993). Since the k value determined from FWD test represents a dynamic value, it is referred to here as $k_{\text{FWD-Dynamic}}$. Deflections obtained from four sensors (D_0 , D_2 , D_4 , and D_5 shown in Figure 10) were used in the AREA₄ calculation. The AREA method was first proposed by Hoffman and Thompson (1981) for flexible pavements and has since been applied extensively for concrete pavements (Darter et al. 1995). AREA₄ is calculated using Equation 5 and has dimensions of length (in inches), as it is normalized with deflections under the center of the plate (D_0):

$$AREA_4 = 6 + 12 \times \left(\frac{D_2}{D_0} \right) + 12 \times \left(\frac{D_4}{D_0} \right) + 6 \times \left(\frac{D_5}{D_0} \right) \quad (5)$$

where D_0 = deflections measured directly under the plate (in.); D_2 = deflections measured at 305 mm (12 in.) away from the plate center (in.); D_4 = deflections measured at 610 mm (24 in.) away from the plate center (in.); and D_5 = deflections measured at 914 mm (36 in.) away from the plate center (in.). The AREA₄ method can also be calculated using different sensor configurations and setups, (i.e., using deflection data from 3, 5, or 7 sensors), and those methods are described in detail in the literature (Substad et al. 2006, Smith et al. 2007)

In early research conducted using the AREA method, the ILLI-SLAB finite element program was used to compute a matrix of maximum deflections at the plate center and the AREA values by varying the subgrade k , the modulus of the PCC layer, and the thickness of the slab (ERES Consultants, Inc. 1982). Measurements obtained from FWD tests were then compared with the ILLI-SLAB program results to determine the k values through back calculation. Barenberg and Petros (1991) and Ioannides (1990) proposed a forward solution procedure based on Westergaard's solution for loading on an infinite plate to replace the back calculation procedure. This forward solution presented a unique relationship between AREA value (for a given load and

sensor arrangement) and the dense liquid radius of relative stiffness (L) in which subgrade is characterized by the k value. The radius of relative stiffness (L) is estimated using Equation 6:

$$L = \left[\frac{\ln\left(\frac{x_1 - AREA_4}{x_2}\right)}{x_3} \right]^{x_4} \quad (6)$$

where $x_1 = 36$, $x_2 = 1812.279$, $x_3 = -2.559$, $x_4 = 4.387$. It must be noted that the x_1 to x_4 values vary with the sensor arrangement and these values are only valid for the AREA₄ sensor setup. Once, the L value is known, the $k_{FWD-Dynamic}$ value can be estimated using Equation 7:

$$k_{FWD-Dynamic} (pci) = \frac{PD_0^*}{D_0 L^2} \quad (7)$$

where P = applied load (lbs), D_0 = deflection measured at plate center (inches), and D_0^* = non-dimensional deflection coefficient calculated using Equation 8:

$$D_0^* = a \cdot e^{-be^{-cL}} \quad (8)$$

where $a = 0.12450$, $b = 0.14707$, $c = 0.07565$. It must be noted that these equations and coefficients are valid for an FWD setup with an 11.81 in. diameter plate.

The advantages of the AREA₄ method are the ease of use without back calculations and the use of multiple sensor data. The disadvantages are that the process assumes that the slab and the subgrade are horizontally infinite. This assumption leads to underestimating the k values of jointed pavements. Croveti (1994) developed the following slab size corrections for a square slab that is based on finite element analysis conducted using the ILLI-SLAB program and is for use in the $k_{FWD-Dynamic}$:

$$Adjusted D_0 = D_0 \left(1 - 1.15085e^{-0.71878\left(\frac{L'}{L}\right)^{0.80151}} \right) \quad (9)$$

$$Adjusted L = L \left(1 - 0.89434e^{-0.61662\left(\frac{L'}{L}\right)^{1.04831}} \right) \quad (10)$$

where L' = slab size (smaller dimension of a rectangular slab, length or width). This procedure also has limitations: (1) it considers only a single slab with no load transfer to adjacent slabs, and (2) it assumes a square slab. The square slab assumption is considered to produce sufficiently

accurate results when the smaller dimension of a rectangular slab is assumed as L' (Darter et al. 1995). Darter et al. 1995 suggested using $L' = \sqrt{Length \times Width}$ to further refine slab size corrections. However, no established procedures for correcting for load transfer to adjacent slabs have been reported so accounting for load transfer remains as a limitation of this method.

AASHTO (1993) suggests dividing the $k_{\text{FWD-Dynamic}}$ value by a factor of 2 to determine the equivalent $k_{\text{FWD-Static}}$ value. The origin of this factor 2 dates back to Foxworthy's work in the 1980s. Foxworthy (1985) reported comparisons between the $k_{\text{FWD-Dynamic}}$ values obtained using Dynatest model 8000 FWD and the Static k values (Static k_{PLT}) obtained from 30 in. diameter plate load tests (the exact procedure followed to calculate the Static k_{PLT} is not reported in Foxworthy 1985). Foxworthy used the AREA based back calculation procedure using the ILLI-SLAB finite element program. Results obtained from Foxworthy's study (Figure 12) are based on 7 FWD tests conducted on PCC pavements with slab thicknesses varying from about 10 in. to 25.5 in. and plate load tests conducted on the foundation layer immediately beneath the pavement over a 4 ft x 5 ft test area. A few of these sections consisted of a 5 to 12 in. thick base course layer and some did not. The subgrade layer material consisted of CL soil from Sheppard Air Force Base in Texas, SM soil from Seymour-Johnson Air Force Base in North Carolina, and an unspecified soil type from McDill Air Force base in Florida. No slab size correction was performed on this dataset.

Data from Foxworthy (1985) yielded a logarithmic relationship between the dynamic and the static k values. On average, the $k_{\text{FWD-Dynamic}}$ values were about 2.4 times greater than the Static k_{PLT} values. Darter et al. (1995) indicated that the factor 2 is reasonable based on results from other test sites (Figure 12). Darter et al. (1995) also compared FWD test data from eight long-term pavement performance (LTPP) test sections with the Static k_{PLT} values and reported factors ranging from 1.78 to 2.16, with an average of about 1.91. The $k_{\text{FWD-Dynamic}}$ values used in that comparison were corrected for slab size. For the analysis conducted in this research project, the corrected $k_{\text{FWD-Dynamic}}$ values (for finite slab size) were divided by 2 and are reported as $k_{\text{FWD-Static-Corr}}$ values.

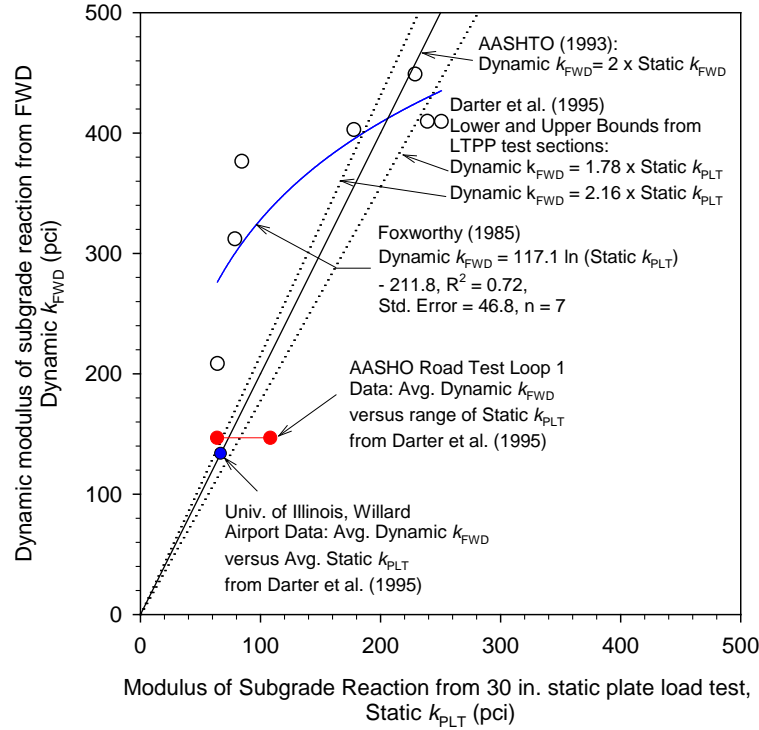


Figure 12. Static k_{PLT} values versus k_{FWD} -Dynamic measurements reported in literature

For tests conducted on the CTB layer, a composite modulus value (E_{FWD-K3}) was calculated using the measured deflection at the center of the plate (D_0), corresponding applied contact force, and Equation 10.

$$E = \frac{(1 - \eta^2) \sigma_0 r}{D_0} \times F \quad (10)$$

where E = elastic modulus (MPa);

D_0 = measured deflection under the plate (mm);

η = Poisson's ratio (0.4);

σ_0 = applied stress (MPa);

r = radius of the plate (mm); and

F = shape factor depending on stress distribution. Assumed as 2 because the plate used in this study is a four-segmented plate, and therefore and produces an assuming a uniform stress distribution according to the manufacturer (see Vennapusa and White 2009).

The subgrade layer modulus (E_{SG}) was determined using Equation 11, per AASHTO (1993):

$$E_{SG} = \frac{(1 - \eta^2) \sigma_0 r^2}{d_i D_i} \quad (11)$$

where: D_i = measured deflection at distance d_i (mm); and d_i = radial distance of the sensor away from the center of the loading plate.

AASHTO (1993) suggests that the d_i must be far enough away that it provides a good estimate of the subgrade modulus, independent of the effects of any layers above, but also close enough that it does not result in a too small value. A graphical solution is provided in AASHTO (1993) to estimate the minimum radial distance based on an assumed effective modulus of all layers above the subgrade and the d_0 value. Salt (1998) indicated that if E_{SG} values are plotted against radial distance, in linear elastic materials such as sands and gravels, the modulus values decrease with increasing distance and then level off after a certain distance. The deformations at the distance at which the modulus values level off can be used to represent E_{SG} . In some cases the modulus values decrease and then increase with distance. Such conditions represent either soils with moderate to high moduli with poor drainage at the top of the subgrade or soft soils with low moduli. In those cases the distance where the modulus is low is represented as E_{SG} .

Ullidtz (1987) described Odemark's method of equivalent thickness (MET) concept and is used in AASHTO (1993). According to the MET concept, a two-layered system with the top layer modulus higher than the bottom layer, can be transformed into a single layer of equivalent thickness with properties of the bottom layer. Using this concept and the modulus of the bottom layer (E_{SG}), the top layer modulus (E_{SB}) can be back-calculated.

In this study, tests conducted on the CTB layer were used to calculate E_{SG} and back-calculate E_{SB} values.

Dynamic Cone Penetrometer

DCP tests were performed in accordance with ASTM D6951-03 *Standard Test Method for Use of the Dynamic Cone Penetrometer in Shallow Pavement Applications* to determine dynamic penetration index (DPI) and calculate California bearing ratio (CBR) using Equation 11.

$$\text{CBR} = \frac{292}{\text{DPI}^{1.12}} \quad (12)$$

The DCP test results are presented in this report as CBR with depth profiles.

Determination of R values

The Resistance Value (R-Value) is a material stiffness parameter that was developed by F.N. Hveem and R.M. Carmany of the California Division of Highways and was first reported in the late 1940s. Rigid pavement thickness design per the CalTrans Highway Design Manual is based on R-Value, so R-Values were determined in this study for reference. Correlations between elastic/resilient modulus and R-Value were provided by Hveem and Carmany (1948) and are

shown in Appendix A. The E_{SG} values calculated from FWD tests were converted to R-Value in this study.

Geostatistical Data Analysis

Spatially referenced in situ point measurements in a dense grid pattern were obtained in this study. These data sets provide an opportunity to quantify “non-uniformity” of compacted fill materials. Non-uniformity can be assessed using conventional univariate statistical methods (i.e., by statistical standard deviation (σ) and coefficient of variation (COV)), but they do not address the spatial aspect of non-uniformity. Vennapusa et al. (2010) demonstrated the use of semivariogram analysis in combination with conventional statistical analysis to evaluate non-uniformity in QC/QA during earthwork construction. A semivariogram is a plot of the average squared differences between data values as a function of separation distance, and is a common tool used in geostatistical studies to describe spatial variation. A typical semivariogram plot is presented in Figure 13. The semivariogram $\gamma(h)$ is defined as one-half of the average squared differences between data values that are separated at a distance h (Isaaks and Srivastava 1989). If this calculation is repeated for as many different values of h as the sample data will support the result can be graphically presented as experimental semivariogram, shown as circles in Figure 13. More details on experimental semivariogram calculation procedure are available elsewhere in the literature (e.g., Clark and Harper 2002, Isaaks and Srivastava 1989).

To obtain an algebraic expression for the relationship between separation distance and experimental semivariogram, a theoretical model is fit to the data. Some commonly used models include linear, spherical, exponential, and Gaussian models. A spherical model was used for data analysis in this report. Arithmetic expression of the spherical model and the spherical variogram are shown in Figure 13. Three parameters are used to construct a theoretical semivariogram: sill ($C+C_0$), range (R), and nugget (C_0). These parameters are briefly described in Figure 13.

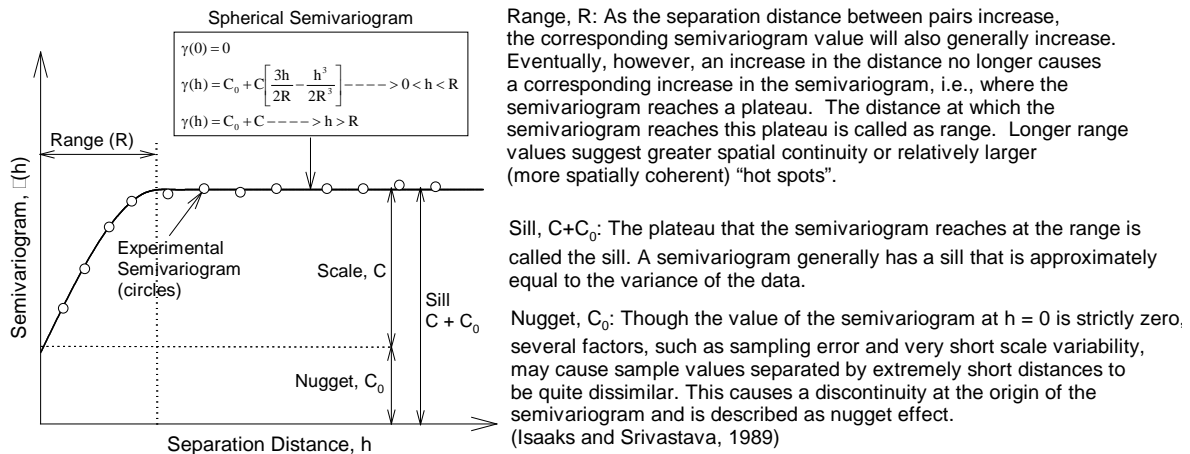


Figure 13. Description and parameters of a typical experimental and spherical semivariogram

Additional discussion on the theoretical models can be found elsewhere in the literature (e.g., Clark and Harper 2002, Isaaks and Srivastava 1989). For the results presented in this report, the sill, range, and nugget values during theoretical model fitting were determined by checking the models for “goodness” using the modified Cressie goodness fit method (see Clark and Harper 2002) and cross-validation process (see Isaaks and Srivastava 1989). From a theoretical semivariogram model, a low sill and longer range of influence values represent the best conditions for uniformity, while the opposite represents an increasingly non-uniform condition.

CHAPTER 5. RESULTS AND ANALYSIS

TS1: CTB Layer

Test measurements obtained from TS1 in a grid pattern with 44 tests over a plan area of about 33 m x 2.5 m provided a dataset to characterize the spatial characteristics of the measurements using geostatistical analysis. Kriged spatial contour maps, semivariograms, histograms of FWD measurements, and raw test measurements along each path are presented in Figure 14 to Figure 17. A spherical semivariogram model showed best fit for all the measurements.

DCP tests were conducted at five test locations. DCP-CBR and cumulative blows with depth profiles are presented in Figure 18. Results indicated that the subgrade layer CBR was relatively high (30 to 100+).

Results indicated that the average composite modulus was about 357 MPa with a COV of about 17%. The average CTB layer modulus was about 7,200 MPa with a COV of about 42%. The average subgrade layer modulus was about 105 MPa with a COV of about 10%, which represents relatively stiff subgrade conditions, which was also confirmed with DCP tests. The average R-value of the subgrade was about 45 with a COV of about 5%.

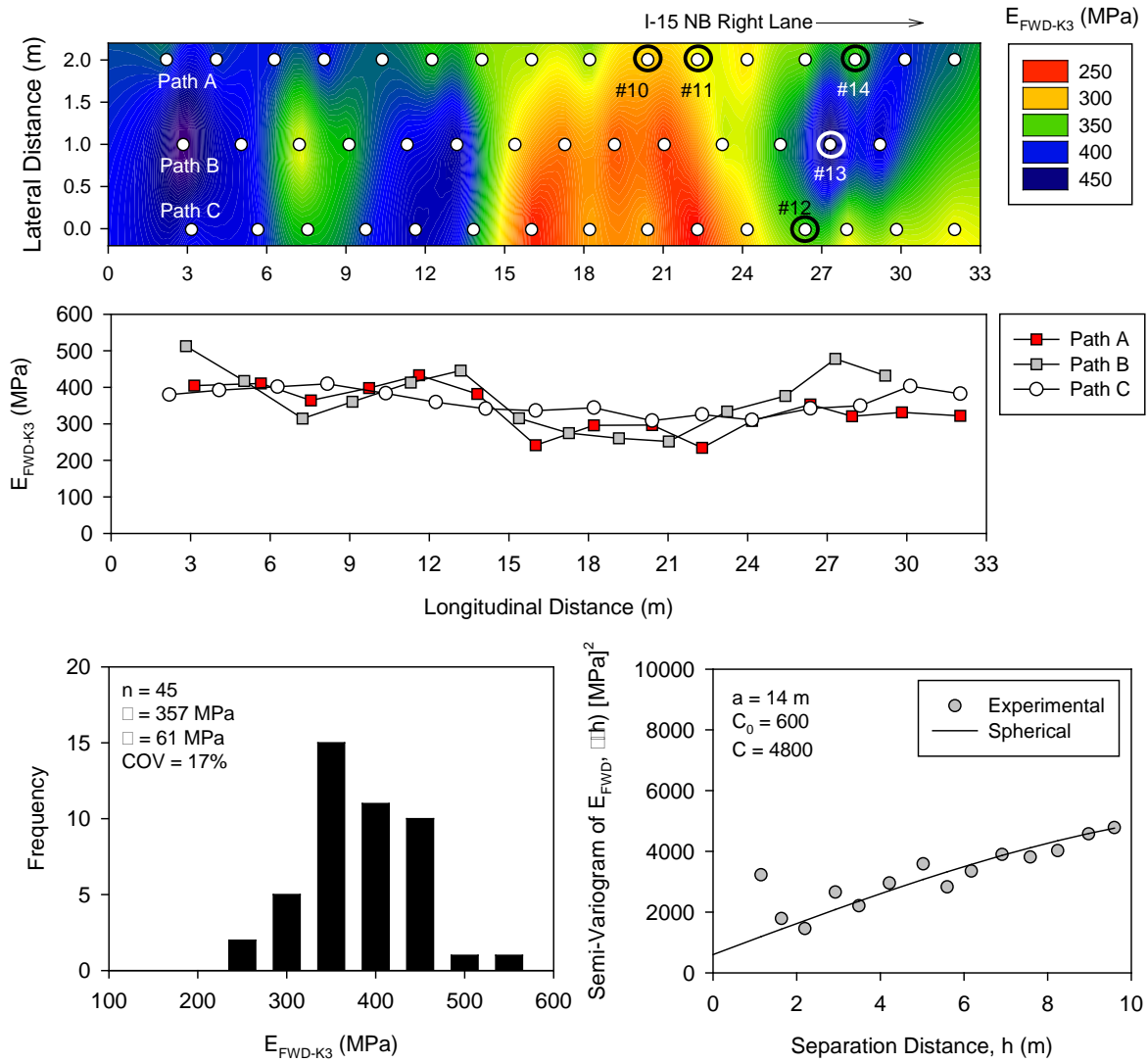


Figure 14. TS1 CTB: Kriged spatial contour map (top), measurements longitudinally along the test section (middle), histogram (bottom left), and semivariogram (bottom right) of E_{FWD-K3} measurements

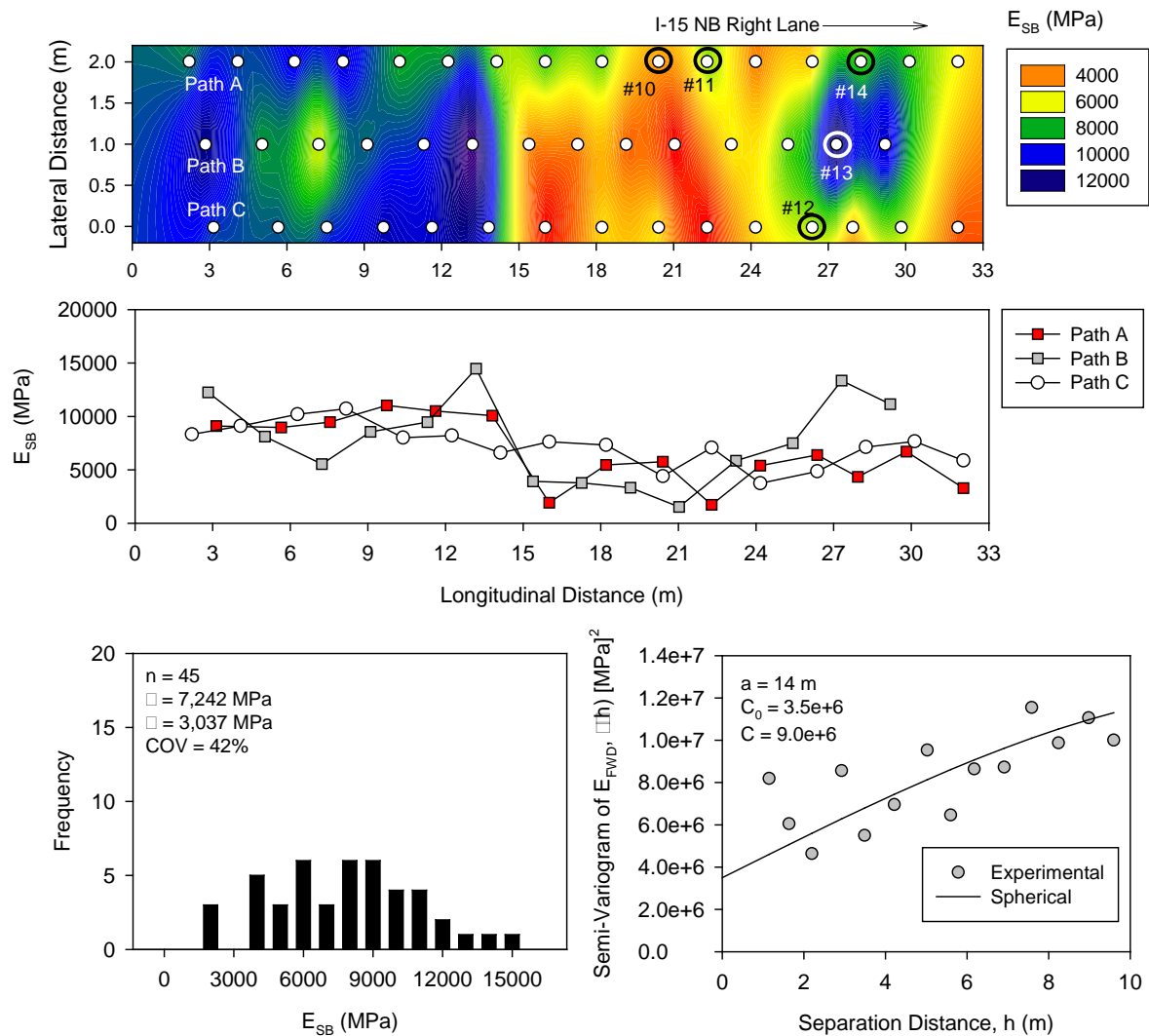


Figure 15. TS1 CTB: Kriged spatial contour map (top), measurements longitudinally along the test section (middle), histogram (bottom left), and semivariogram (bottom right) of E_{SB} (CTB layer modulus) measurements

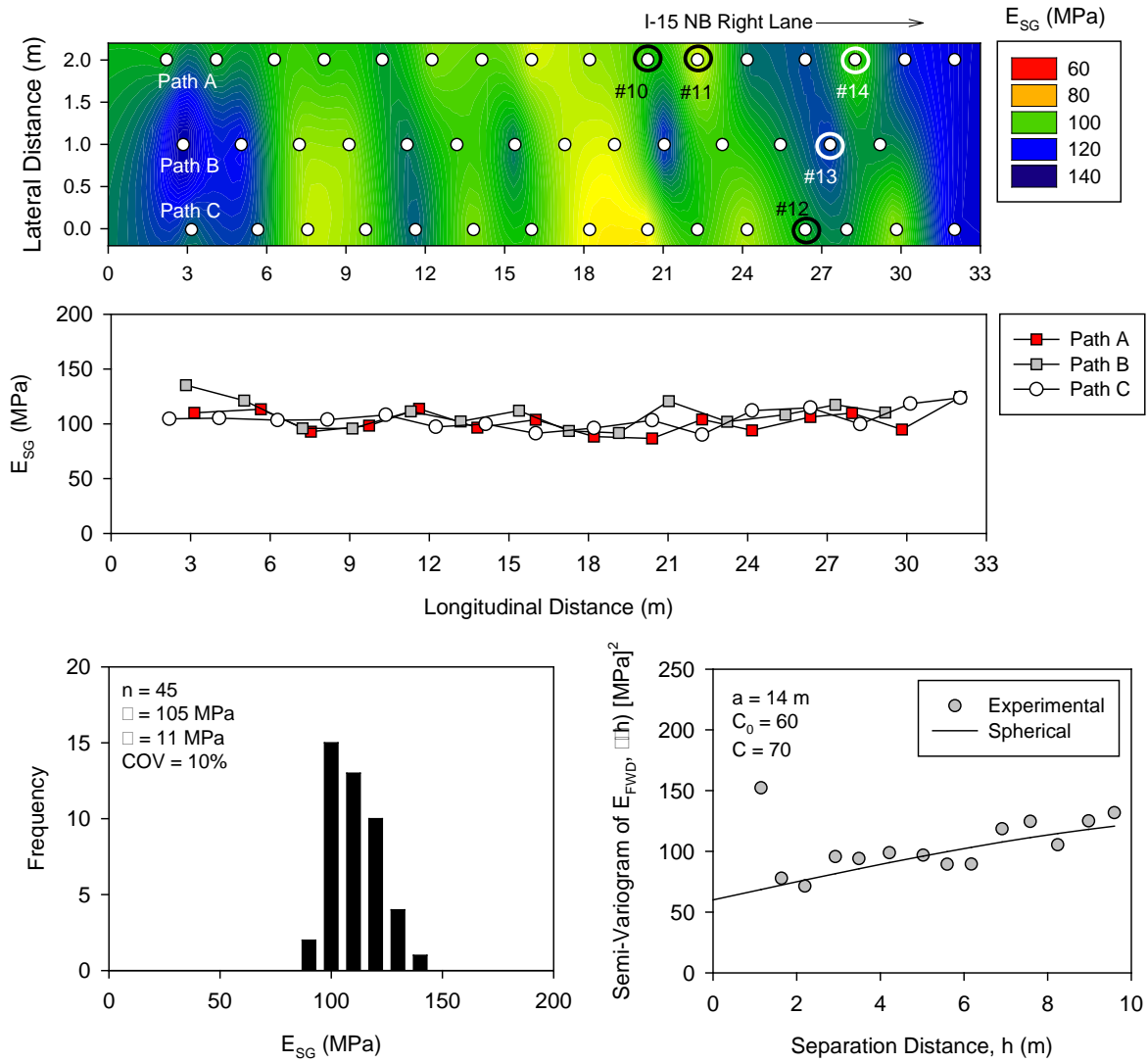
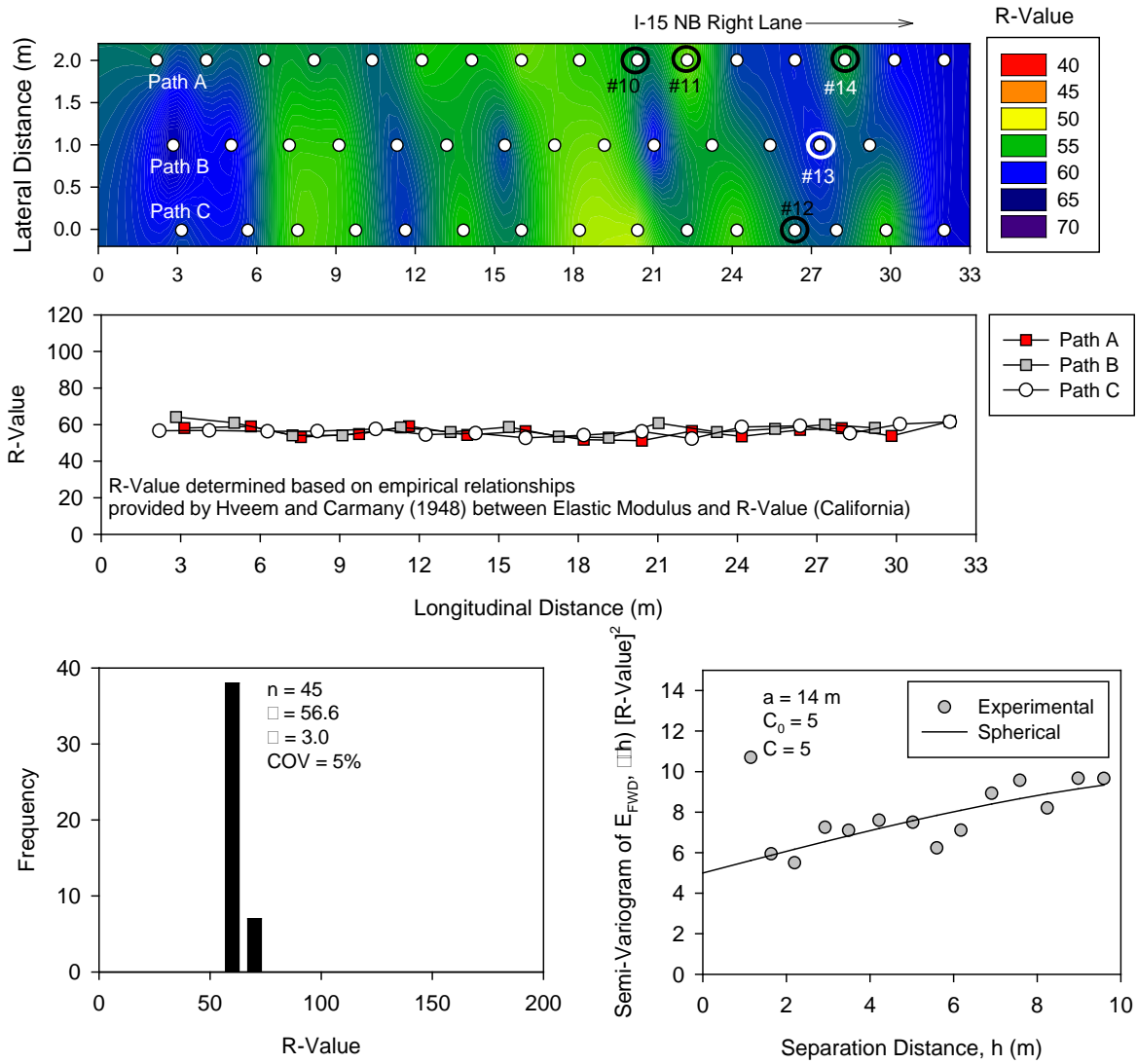


Figure 16. TS1 CTB: Kriged spatial contour map (top), measurements longitudinally along the test section (middle), histogram (bottom left), and semivariogram (bottom right) of E_{SG} (subgrade layer modulus) measurements



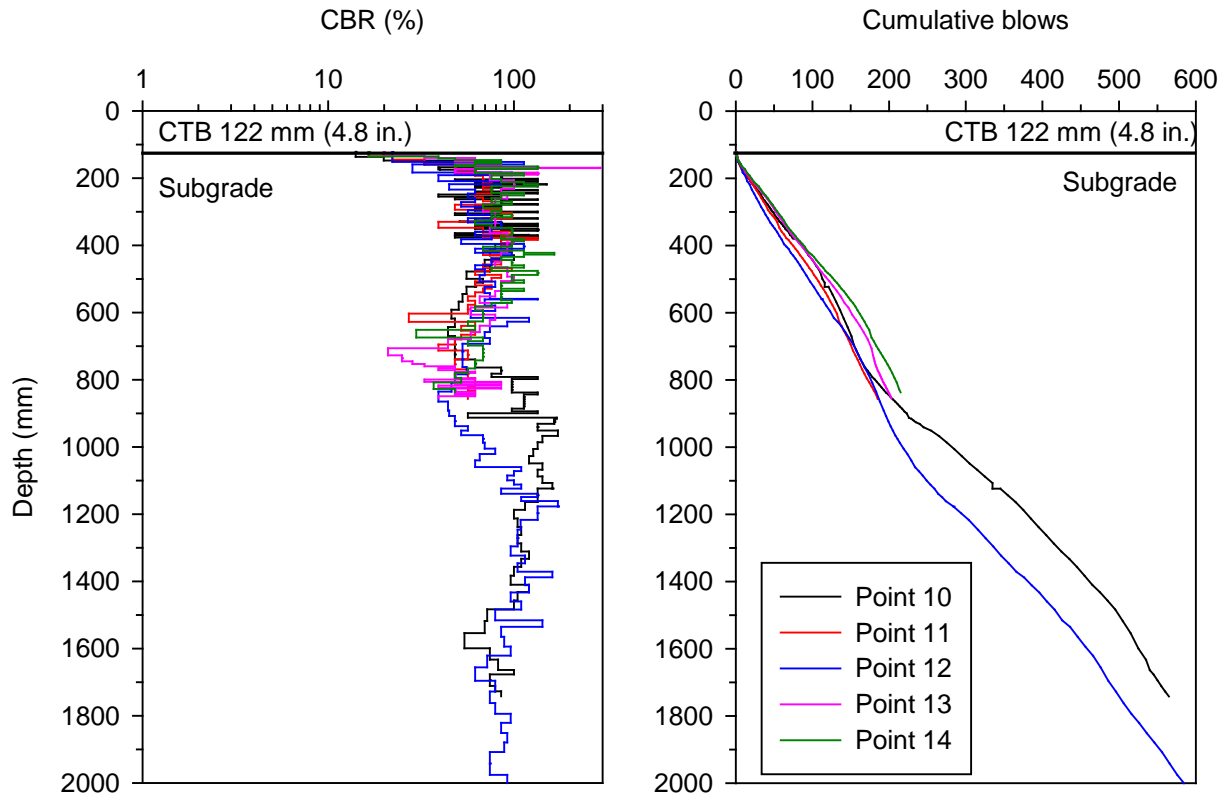


Figure 18. TS1 CTB: DCP-CBR and cumulative blows with depth profiles at 5 test locations

TS2 and TS3: New PCP and Old Pavement

All FWD test results presented below were normalized to a 40 kN (9,000 lb) load. FWD plate deflections (D_0) near mid-panel and joint, and LTE at joints comparing measurements on TS2 and TS3 are presented in Figure 19. Similarly, k and R-values from FWD measurements are provided in Figure 23. The k values were converted to R-values using correlations presented in PCA (1984). FWD deflection basin parameter results (I, AF, SCI, BCI, and BDI) are presented in Figure 21.

Box plots comparing results obtained on PCP and old pavement for measurements at mid-panel and at joint are presented in Figure 22 and Figure 23. Student t-test analysis was conducted to assess if there was any statistically significant differences between measurements obtained on the new and old pavement. The t-test analysis results are summarized in Tables 2 and 3.

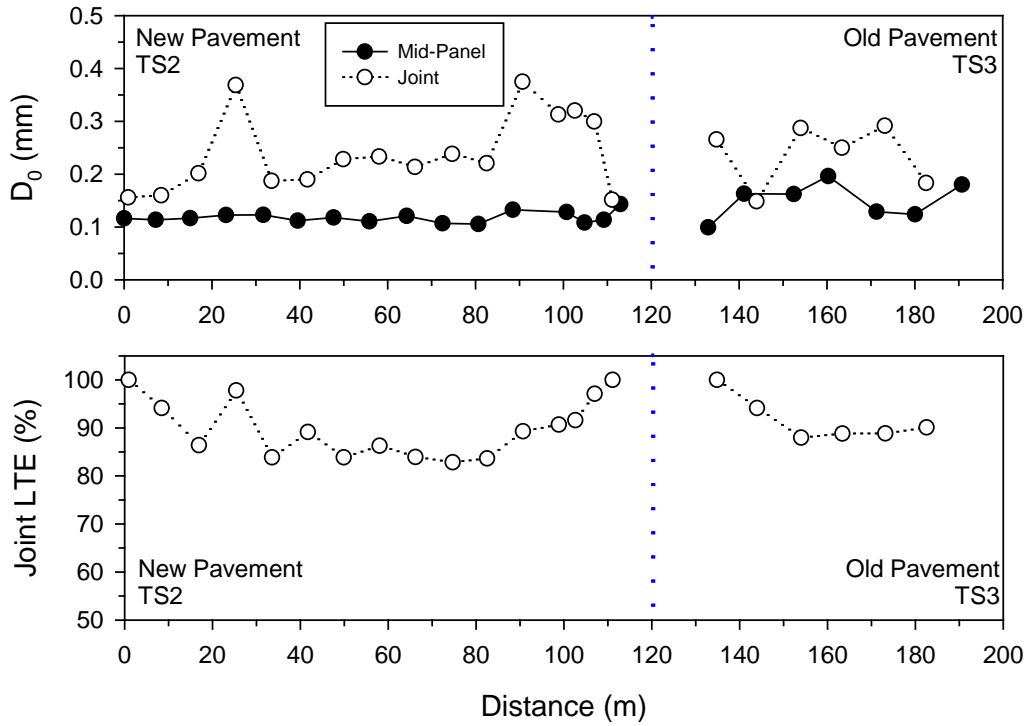


Figure 19. TS2 and TS3: FWD D_0 and joint LTE

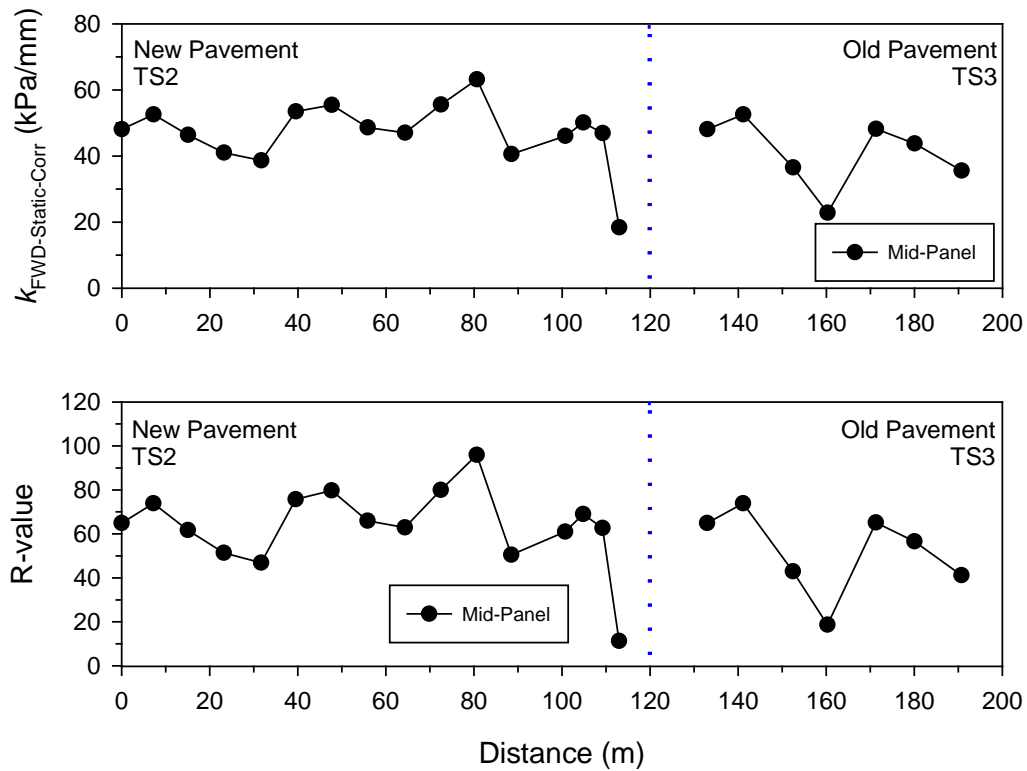


Figure 20. TS2 and TS3: FWD k values and R-value calculated from k value per PCA 1984

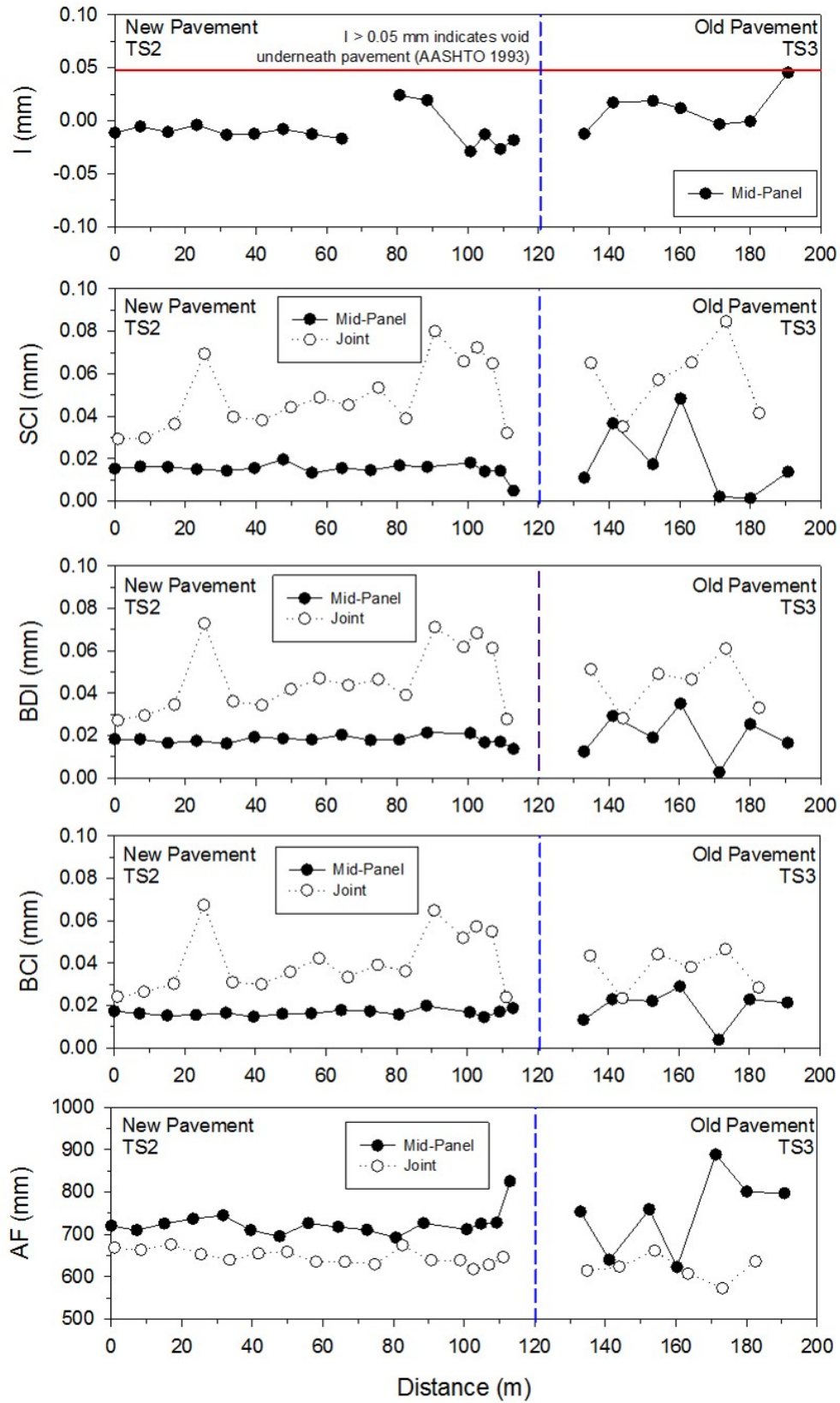


Figure 21. TS2 and TS3: FWD deflection basin parameters

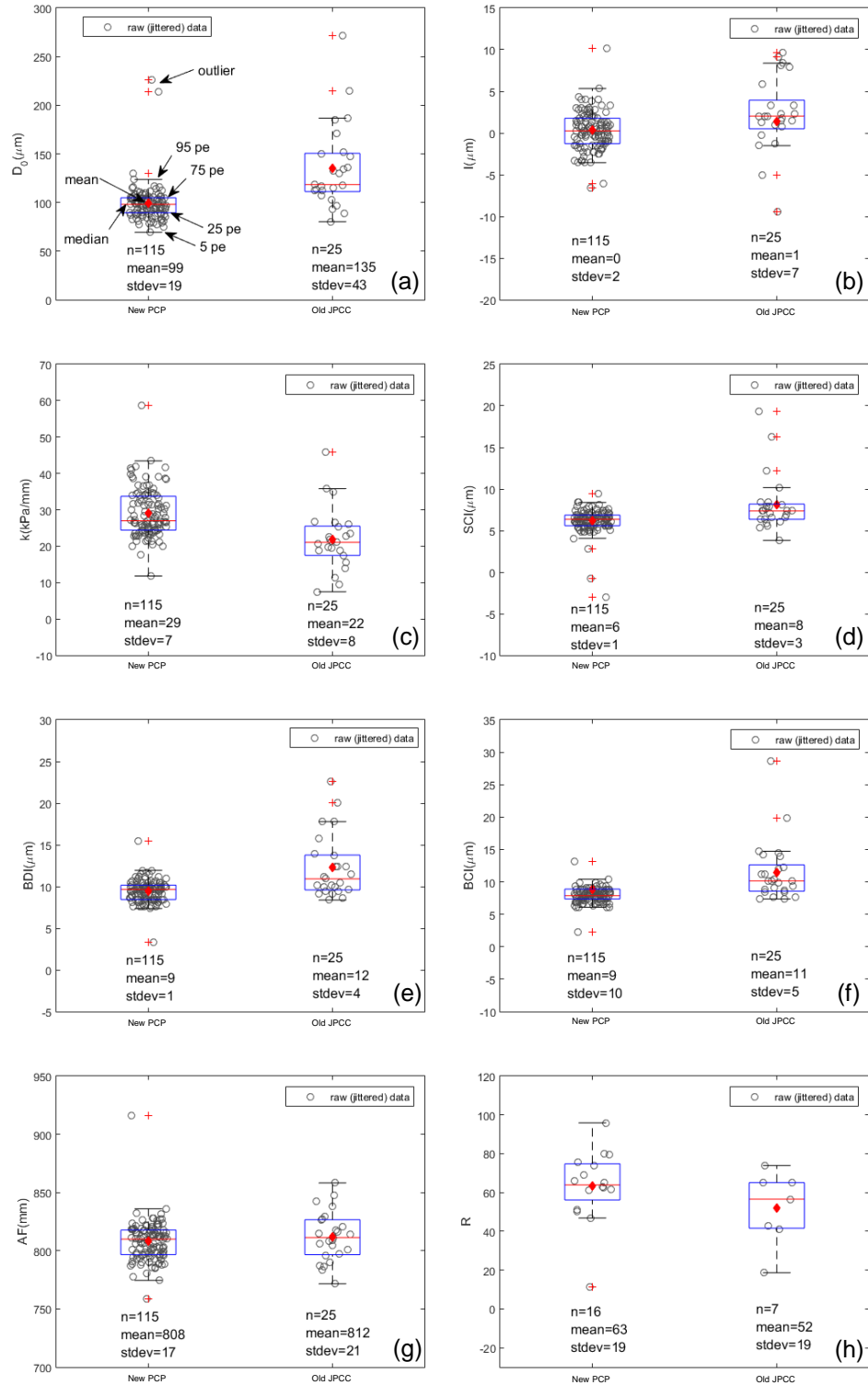


Figure 22. TS2 and TS3: Box plots comparing measurements on new PCP and old pavement for tests conducted near mid-panel: (a) D_0 , (b) I-value, (c) $k_{FWD-Static-Corr}$, (d) SCI, (e) BDI, (f) BCI, (g) Area Factor, and (h) R-value

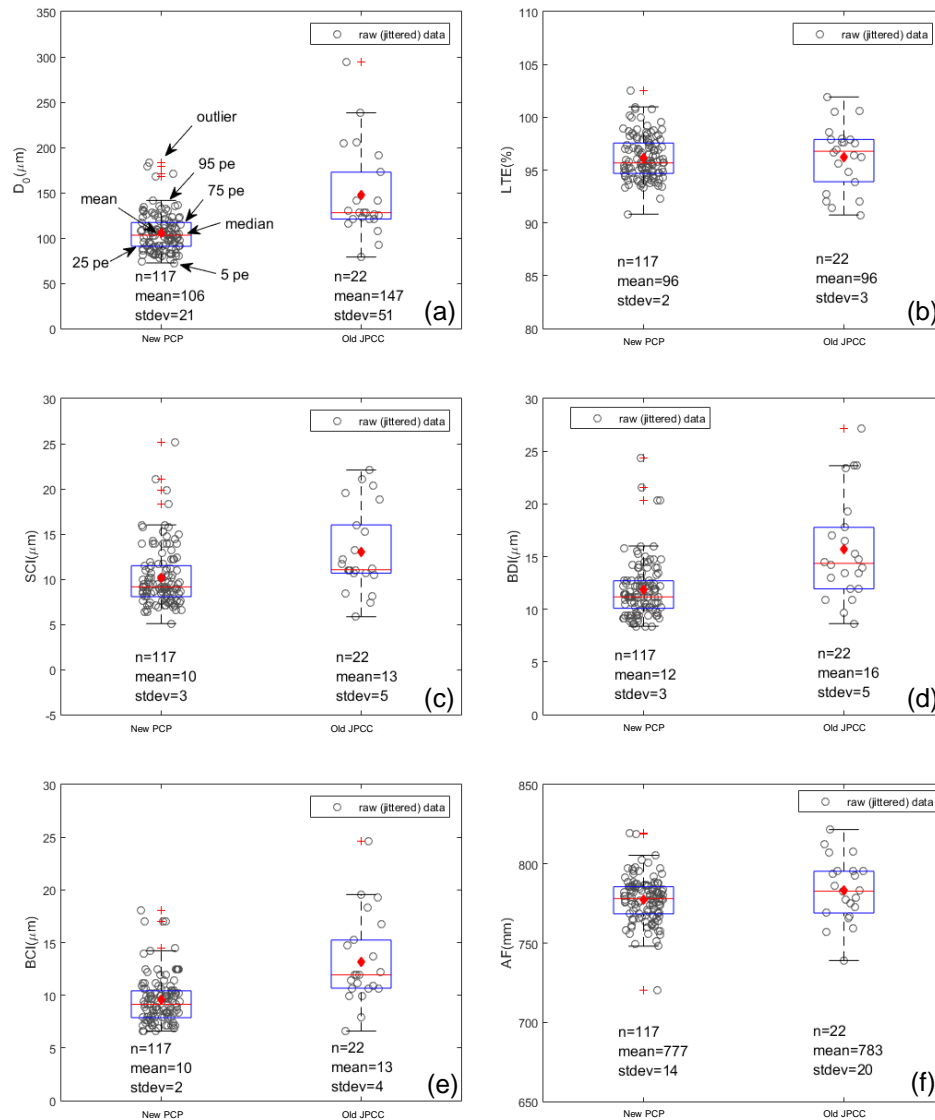


Figure 23. TS2 and TS3: Box plots comparing measurements on new PCP and old pavement for tests conducted near joint: (a) D_0 , (b) LTE, (c) SCI, (d) BDI, (e) BCI, and (f) Area Factor

Results indicated that there was statistically significant difference in D_0 and I values near mid-panel, but not in any of the other deflection basin parameters (SCI, BCI, BDI, AF) and k value. The D_0 and I values were lower on the new pavement than on the old pavement. This suggests that there was improvement in the deflection response near the surface, which reflect better support conditions directly beneath the new pavement. Deeper improvements are not expected and are reflected in the deflection basin parameters.

There were no statistically significant differences in any of the measurement values obtained at the joint. The LTE values were relatively high ($> 85\%$) at all locations. The average R-value

obtained from FWD testing was about 50 and was similar to the value obtained from FWD testing on the CTB layer (45).

Table 2. Summary of t-test analysis on FWD deflection basin parameters near mid-panel on new versus old pavement

Parameter	New or old pavement	Mean	COV (%)	t-value	P _r
D ₀ (μm)	New	118	9	-2.45	0.025
	Old	150	23		
I (μm)	New	-16	-192	-2.56	0.010
	Old	11	174		
k _{FWD-Static-Corr} (kPa/mm)	New	47	21	1.30	0.11
	Old	41	25		
SCI (μm)	New	15	21	-0.48	0.32
	Old	18	99		
BDI (μm)	New	18	11	-0.49	0.32
	Old	20	54		
BCI (μm)	New	17	9	-0.86	0.21
	Old	19	43		
AF (mm)	New	725	4	-0.72	0.25
	Old	751	12		

Note: Highlighted cell indicates statistically significant difference at 95% confidence level between the new and old pavements

Table 3. Summary of t-test analysis on FWD deflection basin parameters near joint on new and old pavement

Parameter	New or old pavement	Mean	COV (%)	t-value	P _r
D ₀ (μm)	New	241	30	0.11	0.46
	Old	238	25		
LTE (%)	New	90	7	-0.67	0.26
	Old	92	7		
SCI (μm)	New	49	33	-1.05	0.16
	Old	58	31		
BDI (μm)	New	46	34	0.25	0.40
	Old	45	27		
BCI (μm)	New	40	35	0.60	0.28
	Old	37	25		
AF (mm)	New	647	3	2.19	0.04
	Old	619	5		

Note: Highlighted cell indicates statistically significant difference at 95% confidence level between the new and old pavements

CHAPTER 6. SUMMARY AND CONCLUSIONS

This report presented field test results and observations from a rehabilitation project on I-15 near Ontario, California, which involved replaced an old pavement with precast concrete pavement (PCP) panels. A total of 730 panels were installed. Unit cost of the PCP for winning bid was about \$418/panel. The total bid cost of the project was about \$51.9 million. PCP systems constituted approximately \$4.6 million of the total construction cost. The existing old pavement was originally constructed in the 1970s with approximately 213 mm (8.4 in.) of PCC over 122 mm (4.8 in. of CTB). The old pavement was removed, a new thin bedding sand layer was placed, and 203 mm (8 in.) thick new PCP panels were placed as part of the rehabilitation work. Bedding grout was pumped into precast ports for undersealing and dowel grout was injected to the dowel slots.

Following are some key findings from work performed by the SHRP2 R05 research team and CalTrans:

- FWD testing was conducted by Tayabji et al. (2013a) on PCP panels constructed with and without bedding grout. The results showed that deflections were considerably smaller (3 to 5 mils) on panels where bedding grout was used.
- The panels with only dowel-slot grouting showed more variability in surface deflections.
- Field monitoring several months after construction showed thin hair-line cracks on several panels. A detailed survey was conducted on 696 panels, of which 24% were cracked.
- Based on crack survey mapping and field notes during construction, it was concluded that the contractor's grading practices contributed to the cracking. It was found that the stringline approach used to place the bedding material sometimes created high and low spots resulting in non-uniform support conditions. Cracks at some locations were attributed to opening the lane to traffic before grouting.

The ISU research team was present on site on June 28, 2010 to monitor construction operations and conduct field testing. Kuab FWD and DCP tests were conducted on CTB layer, and FWD tests were conducted on two adjacent test sections consisting of old pavement and new PCP panels. Following are some key findings from the ISU testing:

- Tests on the CTB layer indicated that the average composite modulus was about 357 MPa with a COV of about 17%. The average CTB layer modulus was about 7,200 MPa with a COV of about 42%. The average subgrade layer modulus was about 105 MPa with a COV of about 10%, which represented relatively stiff subgrade conditions.
- CBR values estimated in the subgrade from DCP tests showed relatively high values (ranging between 30 and 100), which confirms the relatively high subgrade modulus values. The average R-value of the subgrade was about 45 with a COV of about 5%.
- Statistical analysis of FWD measurement values obtained on the old and new pavement indicated that there was a statistically significant difference in surface

deflection (D_0) and zero-load intercept (I) values near mid-panel, but not in any of the other deflection basin parameters and the modulus of subgrade reaction (k) value. The D_0 and I values were lower on the new pavement than on the old pavement. This suggests that there was improvement in the deflection response near the surface, which reflects better support conditions directly beneath the new pavement. This was also confirmed in the SHRP2 R05 testing. Deeper improvements are not expected which is reflected in the deflection basin parameters.

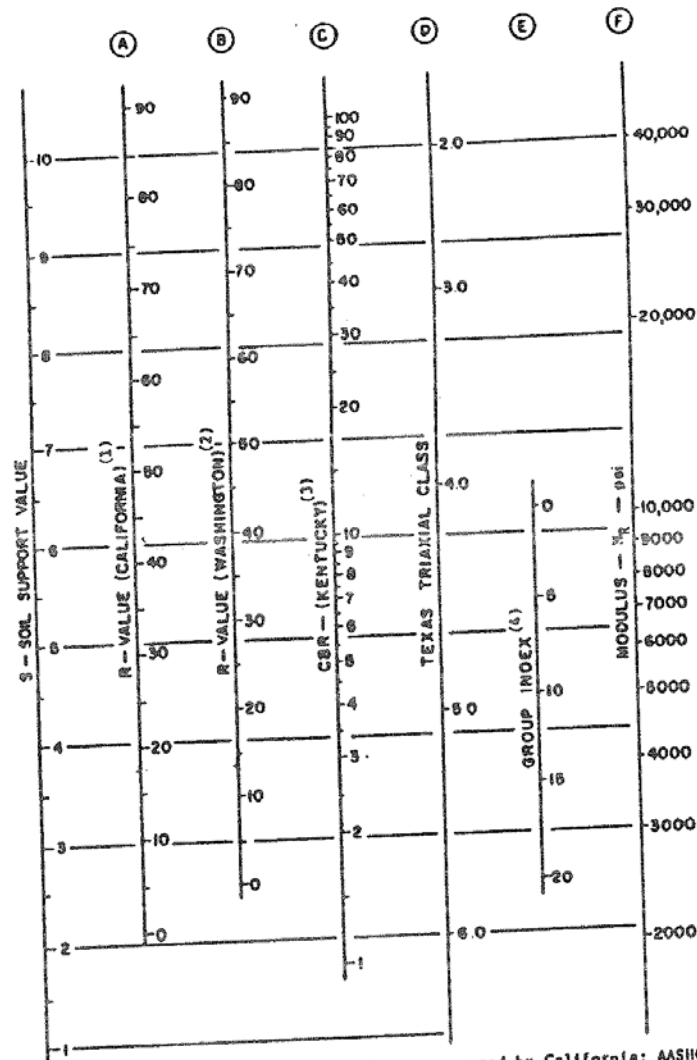
- There were no statistically significant differences in any of the measurement values obtained at the joint. The LTE values were relatively high (> 85%) at all locations.
- The average R-value obtained from FWD testing was about 50 and was similar to the value obtained from FWD testing on the CTB layer (45).

REFERENCES

- AASHTO. (1993). *AASHTO design guide for design of pavement structures*. American Association of State Highway and Transportation Officials, Washington DC.
- ASTM D4694-09. (2009). “Standard Test Method for Deflections with a Falling-Weight-Type Impulse Load Device.” American Standards for Testing Methods (ASTM), West Conshohocken, PA.
- ASTM D6951-03. (2010). “Standard test method for use of the dynamic cone penetrometer in shallow pavement applications.” American Standards for Testing Methods (ASTM), West Conshohocken, PA.
- Barenberg, E. J., and Petros, K. A. (1991). Evaluation of Concrete Pavements Using NDT Results, Illinois Highway Research Project IHR-512, University of Illinois and Illinois Department of Transportation, Report No. UILU-ENG-91-2006, IL.
- Clark, I., and Harper, W. (2002). *Practical geostatistics 2000*. 3rd reprint, Ecosse North America LLC, Columbus, Ohio.
- Crovetti, J. A. (1994). “Design and evaluation of jointed concrete pavement systems incorporating open-graded bases.” Ph.D. Dissertation, University of Illinois at Urbana-Champaign, IL.
- Darter, M. I., Hall, K. T., and Kuo, C-M. (1995). Support under Portland Cement Concrete Pavements, NCHRP Report 372, Transportation Research Board, Washington, D.C.
- ERES Consultants, Inc. (1982). Nondestructive Structural Evaluation of Airfield Pavements, Prepared for U.S. Army Corps of Engineering Waterways Experiment Station, Vicksburg, MS.
- Foxworthy, P.T. (1985). “Concepts for the development of a nondestructive testing and evaluation system for rigid airfield pavements.” Ph.D. Thesis, University of Illinois at Urbana-Champaign, IL.
- Hartog, J. (2012). *I-15 Precast Pavement Installation: Construction Report*, CalTrans Report EA 08-472214, CalTrans District 8, San Bernardino, CA.
- Hoffman, M.S., and Thompson, M.R. (1981). Mechanistic Interpretation of Nondestructive Pavement Testing Deflections. Transportation Engineering Series No. 32, Illinois Cooperative Highway and Transportation Research Series No. 190, University of Illinois at Urbana-Champaign, Champaign, IL.
- Horak, E. (1987). Aspects of deflection basin parameters used in a mechanistic rehabilitation design procedure for flexible pavements in South Africa. PhD Dissertation, University of Pretoria, South Africa.
- Hveem, F. N., and Carmany, R. M. (1948). “The factors underlying the rational design of pavements,” *Proceedings, Highway Research Board*, Vol. 28, pp. 101–136.
- Ioannides, A. M. (1990). “Dimensional analysis in NDT rigid pavement evaluation”, *Transportation Engineering Journal*, ASCE, Vol. 116, No. TE1
- Isaaks, E. H., and R. M. Srivastava. (1989). *An introduction to applied geostatistics*. Oxford University Press, New York.
- Janssen, D. J., and Snyder, M. B. (2000). “Temperature-moment concept for evaluating pavement temperature data.” *Journal of Infrastructure Systems*, 6(2), 81–83.
- Kilareski, W. P., and Anani, B. A. (1982). Evaluation of In Situ Moduli and Pavement Life from Deflection Basins. Fifth International Conference of Asphalt Pavements, University of Michigan, Ann Arbor, MI.

- Kohler, E., Theyse, H., and du Plessis, L. (2007). "Interim assessment of expected structural life of pre-cast concrete pavement slabs," UCPRC-TM-2007-04, University of California Pavement Research Center, UC Davis and Berkeley, California.
- Salt, G. (1998). "Pavement Deflection Measurement and Interpretation for the Design of Rehabilitation Treatments." Transit New Zealand Report, 117.
- Smith, K. D., Wade, M. J., Bruinsma, J. E., Chatti, K., Vandenbossche, J. M., Yu, H. T., Hoerner, T. E., Tayabji, S. D. (2007). Using Falling Weight Deflectometer Data with Mechanistic-Empirical Design and Analysis, Draft Interim Report, DTFH61-06-C-0046, Federal Highway Administration, Washington, D.C.
- Substad, R. N. (2002). *LTPP Data Analysis: Feasibility of Using FWD Deflection Data to Characterize Pavement Construction Quality*. NCHRP Web Document 52, Project No. 20-50(9), National Cooperative Highway Research Program, Transportation Research Board of the National Academies, Washington, DC.
- Substad, R. N., Jiang, Y. J., and Lukanen, E. O. (2006). Guidelines for Review and Evaluation of Backcalculation Results, FHWA-RD-05-152, Federal Highway Administration, Washington, D.C.
- Tayabji, S., D. Ye, and N. Buch. (2013a). *Precast Concrete Pavement Technology*. SHRP 2 Report No. S2-R05-RR-1, Strategic Highway Research Program, Transportation Research Board of the National Academies, Washington, DC.
- Tayabji, S., Ye, D., and Buch, N. (2013b) "Precast Concrete Pavements: Technology Overview and Technical Considerations," *PCI Journal*, 112–128.
- Ullidtz, P. (1987). *Pavement analysis*, Developments in Civil Engineering Series, Elsevier, New York.
- van Til, C. J., McCullough, B. F., Vallerga, B. A., and R. G. Hicks. (1972). *Evaluation of AASHTO Interim Guides for Design of Pavement Structures*. NCHRP 128, Highway Research Board.
- von Quintus, H. L., and Simpson, A. L. (2002). Backcalculation of Layer Parameters for LTPP Test Sections, Volume II: Layered Elastic Analysis for Flexible and Rigid Pavements, Research Report, Long-Term Pavement Performance Program, Report No. FHWA-RD-01-113, Federal Highway Administration, Washington, DC, October 2002.
- Vandenbossche, J. M. (2005). "Effects of slab temperature profiles on the use of falling weight deflectometer data to monitor joint performance and detect voids." *Transportation Research Record: Journal of the Transportation Research Board*. No. 2005, Transportation Research Board of the National Academies, Washington, DC, pp. 75–85.
- Vennapusa, P., and White, D. J. (2009). "Comparison of light weight deflectometer measurements for pavement foundation materials." *Geotechnical Testing Journal*, ASTM, 32(3), 239–251.
- Vennapusa, P., White, D. J., and Morris, M. (2010). "Geostatistical analysis of spatial referenced roller-integrated compaction measurements." *Journal of Geotechnical and Geoenvironmental Engineering*, ASCE, 136(6), 813–822.

APPENDIX: CORRELATIONS BETWEEN R-VALUE AND MODULUS



- (1) The correlation is with the design curves used by California; AASHTO designation is T-173-60, and exudation pressure is 240 psi. See Ivey, F.M., and Carmany, R.H., "The Factors Underlying the Rational Design of Pavements." *Proc. HRB*, Vol. 28 (1948) pp. 101-136.
- (2) The correlation is with the design curves used by Washington Dept. of Highways; exudation pressure is 300 psi. See "Flexible Pavement Design Correlation Study." *HRB Bull.* 133 (1956).
- (3) The correlation is with the CBR design curves developed by Kentucky. See Drake, W.B., and Havens, J.H., "Re-Evaluation of Kentucky Flexible Pavement Design Criterion." *HRB Bull.* 233 (1959) pp. 33-56. The following conditions apply to the laboratory-modified CBR: specimen is to be molded at or near the optimum moisture content as determined by AASHTO T-99; dynamic compaction is to be used with a hammer weight of 10 lb dropped from a height of 18 in.; specimen is to be compacted in five equal layers with each layer receiving 10 blows; specimen is to be soaked for 4 days.
- (4) This scale has been developed by comparison between the California R-value and the Group Index determined by the procedure in *Proc. HRB* Vol. 25 (1945) pp. 376-392.

Figure 24. Chart to estimate resilient modulus (M_r) of subgrade from CBR (from AASHTO 1993 Appendix FF based on results from van Til et al. 1972)